Chapter 2
Environmental Forces

Abstract This chapter deals with different types of environmental loads on offshore structures. It also includes code information regarding the loads. Step-by-step method for load estimate on a cylindrical member and an example structure is detailed. The procedure for estimating wave loads is illustrated through examples. Computer codes are included for load estimates; simple MATLAB program is used to illustrate the code. Exercise is given at the end along with the key for self-learning.

Keywords Wind forces · Wave forces · Aerodynamic admittance function · Current forces · Wave theories · Ice and snow loads · Earthquake loads · Accidental loads · General design requirements

2.1 Introduction

Loads for which an offshore structure must be designed can be classified into the following categories:

- Permanent loads or dead loads
- Operating loads or live loads
- Other environmental loads including earthquake loads
- Construction and installation loads
- Accidental loads

While the design of buildings onshore is influenced mainly by the permanent and operating loads, the design of offshore structures is dominated by environmental loads, especially waves, and the loads arising in the various stages of construction and installation. In civil engineering, earthquakes are normally regarded as accidental loads. But in offshore engineering, they are treated as environmental loads. Environmental loads are those caused by environmental phenomena that are random in nature. These include wind, waves, current, tides, earthquakes, temperature, ice, seabed movement, and marine growth. Their

S. Chandrasekaran, *Dynamic Analysis and Design of Offshore Structures*,
Ocean Engineering & Oceanography 9,
https://doi.org/10.1007/978-981-10-6089-2_2

characteristic parameters, defining design load values, are determined in special studies on the basis of available data. According to U.S. and Norwegian regulations (or codes of practice), the mean recurrence interval for the corresponding design event must be 100 years, while according to the British rules it should be 50 years or greater. The different load to be considered while designing the structure are wind loads, wave load, mass, damping, ice load, seismic load, current load, dead load, live load, impact load, etc.

2.2 Wind Force

Wind forces on offshore structures is caused by complex fluid-dynamics phenomenon, which is generally difficult to calculate with high accuracy. Most widely used engineering approaches to estimate wind forces on offshore structures based on few observations as listed below

- When stream of air flows with constant velocity (v), it will generate force on the flat plate of area (A).
- The plate will be placed orthogonal to the flow direction.
- This force will be proportional to (Av^2).
- The proportionality constant is independent of the area, which is verified by experimental studies.

Hence, the wind force on a plate orthogonal to the wind flow direction can be determined by the net wind pressure as given below

$$p_{\mathrm{w}} = \frac{1}{2}\rho_{\mathrm{a}} C_{\mathrm{w}} v^2 \qquad (2.1)$$

where, ρ_{a} is mass density of air (1.25 kg/m^3), and C_{w} is wind pressure coefficient. It is important to note that the mass density of air increases due to the water spray (splash) up to a height of 20 m above MSL. Hence, the total wind induced force, on the plate is given by:

$$F_{\mathrm{w}} = p_{\mathrm{w}} A \qquad (2.2)$$

If the plate has an angle has an angle (θ) with respect to the wind direction, then the appropriate projected area, normal to the flow direction should be used in the above equation. The wind pressure coefficient C_{w} is determined under controlled stationary wind flow conditions in a wind tunnel. It depends on the Reynolds number; typical values of 0.7–1.2 are used for cylindrical members. Natural wind has two components: (i) mean wind component (which is static component); and (ii) fluctuating, gust component (which is a dynamic component). The gust component is generated by the turbulence of the flow field in all the three spatial directions. For offshore locations, mean wind speed is much greater than the gust component, which means that in most of the design cases, a static analysis will suffice. The wind velocity is given by

$$v(t) = \bar{v} + v(t) \tag{2.3}$$

where, $\bar{v}\sqrt{a^2 + b^2}$ the mean wind velocity and $v(t)$ is the gust component. The spatial dependence of the mean component is only through the vertical coordinate, while $v(t)$ is homogeneous in both space and time. Wind forces in the directions parallel (drag force) and normal to the wind direction (lift force) are given by

$$\begin{aligned} F_\mathrm{D} &= \frac{1}{2}\rho C_\mathrm{D}\bar{v}_\mathrm{z}A \\ F_\mathrm{L} &= \frac{1}{2}\rho C_\mathrm{L}\bar{v}_\mathrm{z}A \end{aligned} \tag{2.4}$$

Wind spectrum above water surface is given by one-seventh power law, which is

$$v_\mathrm{z} = V_{10}\left[\frac{z}{10}\right]^{\frac{1}{7}} \tag{2.5}$$

where, v_z is the wind speed at elevation of z m above MSL, V_{10} is the wind speed at 10 m above MSL, and 10 m is called the reference height. Power law is purely empirical and most widely used. It is tested with the actual field measurements and found to be in good agreement. As Eq. (2.5) gives mean wind component, the gust component can be obtained by multiplying a gust factor with the sustained wind speed. Average gust factor (F_g) is in the range of 1.35–1.45; variation of the gust factor along the height is negligible. The sustained wind speed, which is to be used in the design, is the *one minute average wind speed*, according to the U.S. Weather Bureau. The product of sustained wind speed and the gust factor will give the *fastest mile velocity*. 200 year sustained wind velocity of 125 miles per hour is to be used for the design of offshore structures.

Wind produces a low-frequency excitation. The fluctuating component is modeled probabilistically. Drag force on the members will be caused by the encountered waves and wind. Wave forces alone acting on the member will cause inertia and drag forces, while earthquake forces cause only inertia forces on the members. Hence, vibration of the structure induced by wind and waves are different from that caused by earthquakes. For the design of members under wind loads, most of the international codes prefer quasi-static analysis. Very slender and flexible structures are wind-prone; for members under wave action, de-amplification takes place in flexible structures due to compliancy. While considering wind as a dynamic process, the following parameters are important:

- Length of the record: The record can be continuous, intermittent or select record whose values are above the threshold value. For the record to be continuous, average values of the wind velocity is lesser than that of the intermittent because of the longer length of the record when compared with the former.

- Wind spectrum: It is used as input for the structural analysis, which defines the fluctuating wind component.
- Gust component: It is approximated by the *aerodynamic admittance function*.

2.2.1 Aerodynamic Admittance Function

Aerodynamic admittance function is an intelligent way to define the cross-spectrum in the analysis, indirectly. There are two reasons for using the aerodynamic admittance function: (i) to bypass the rigorous random analysis; and (ii) possibility of an accurate measurement of this function through wind tunnel experiments. In this manner, the spatial variations of wind velocity are handled intelligently in the design. Force due to wind is given by

$$\begin{aligned} F_{\mathrm{w}}(t) &= \frac{1}{2}\rho_{\mathrm{a}} C_{\mathrm{w}} v^2 A \\ &= \frac{1}{2}\rho_{\mathrm{a}} C_{\mathrm{w}} A[\bar{v} + v(t)]^2 \\ &= \frac{1}{2}\rho_{\mathrm{a}} C_{\mathrm{w}} A[\bar{v}^2 + (v(t))^2 + 2\bar{v}v(t)] \\ &\quad \text{by neglecting higher powers of gust component,} \\ &\cong \overline{F}_{\mathrm{w}} + \rho_{\mathrm{a}} C_{\mathrm{w}} A \bar{v} v(t) \end{aligned} \tag{2.6}$$

In the above equation, wind force is expressed as a sum of mean component and the gust component. Wind is considered an ergodic process; the (one-sided) power spectral density of the wind process is then related to the wind spectrum as

$$S_{\mathrm{F}}^{+}(\omega) = [\rho_{\mathrm{a}} C_{\mathrm{w}} A \bar{v}]^2 S_{\mathrm{U}}^{+}(\omega) \tag{2.7}$$

Substituting Eq. (2.2) in Eq. (2.7) and rearranging the terms, we get

$$S_{\mathrm{F}}^{+}(\omega) = \frac{4\left[\overline{F}_{\mathrm{w}}\right]^2}{[\bar{v}]^2}\left[\chi\left\{\frac{\omega\sqrt{A}}{2\pi\bar{v}}\right\}\right]^2 S_{\mathrm{U}}^{+}(\omega) \tag{2.8}$$

In the above equation, force and the response spectra are connected by the *aerodynamic admittance function*, which varies as below

$$\begin{aligned} &\text{for } \frac{\omega\sqrt{A}}{2\pi\bar{v}} \Rightarrow 0, \quad \chi\left\{\frac{\omega\sqrt{A}}{2\pi\bar{v}}\right\} \Rightarrow 1 \\ &\text{for } \frac{\omega\sqrt{A}}{2\pi\bar{v}} \Rightarrow \infty, \quad \chi\left\{\frac{\omega\sqrt{A}}{2\pi\bar{v}}\right\} \Rightarrow 0 \end{aligned} \tag{2.9}$$

Aerodynamic admittance function is found empirically, as proposed below (Davenport 1961):

$$\chi(x) = \left\{ \frac{1}{[1 + (2x)^{4/3}]} \right\} \tag{2.10}$$

2.2.2 *Wind Data*

Wind observations were made for maximum wind speed, mean wind direction, and mean wind speed. The standard wind data represents 10 min average speed measured on mean sea level (DNV 1982). Wind instruments are mounted on light houses, ships, at fixed positions at sea approximately 4 m above sea level. The visual observations were made to find the wind directions. Instrumental wind data are collected by anemometers and the wind directions may also be measured by wind vane.

2.3 Wind Spectra

Wind spectra for the design of offshore structures are listed below with the details. For the reference height of z = 10 m, wind spectra as applied to offshore structures are expressed in terms of circular frequency as given below

$$S_{\mathrm{u}}^{+}(\omega) = fG_{\mathrm{u}}^{+}(f) \tag{2.11}$$

where, $S_{\mathrm{u}}^{+}(\omega)$ is the wind spectral density and f is the frequency.

(i) *Davenport spectrum*

Davenport spectrum is focused on the high-frequency portion of the wind data, with the adjustment of a single site-specific parameter. The power in a frequency band is described by this parameter as a complex function of average wind velocity.

$$\frac{\omega S_{\mathrm{u}}^{+}(\omega)}{\delta \overline{U}_{\mathrm{p}}^{2}} = \frac{4\theta^{2}}{\left(1 + \theta^{2}\right)^{4/3}} \tag{2.12}$$

(ii) *Harris spectrum*

Steady wind forces are calculated from time averaged wind speed. However, fluctuating gust component may lead to resonating oscillations in offshore structures. Harris spectrum considered the spatial correlation of gust effects and mean wind velocity variation. This is not recommended for frequencies less than 0.1 Hz.

$$\frac{\omega S_{\mathrm{u}}^{+}(\omega)}{\delta \overline{U}_{\mathrm{p}}^{2}} = \frac{4\theta}{\left(2+\theta^{2}\right)^{5/6}} \tag{2.13}$$

Derivable variable θ is given by

$$\theta = \frac{\omega L_{\mathrm{u}}}{2\pi \overline{U}_{10}} = \frac{\delta L_{\mathrm{u}}}{\overline{U}_{10}}, \quad 0<\theta<\infty \tag{2.14}$$

where, L_{u} is integral length scale (=1200 m for Davenport and 1800 m for Harris spectrum), δ is surface drag coefficient referred to $\overline{U}_{10}$. For offshore locations, δ = 0.001. $\overline{U}_{10}$ is the mean wind speed at a height of 10 m. It is important to note that none of these spectrum used in the analysis of wind speed is recorded offshore; they are based on onshore records. Hence these applications to offshore locations are questionable. They have serious problem when used for low-frequency flexible structures.

Alternatively, for large floating structures, following spectra are recommended (Dyrbye and Hassen 1997).

(a) *Kaimal spectrum*

Kaimal spectrum may give a better fit to empirical observations of atmospheric turbulence.

$$\frac{\omega S_{\mathrm{u}}^{+}(\omega)}{\sigma_{\mathrm{u}}^{2}} = \frac{6.8\theta}{(1+10.2\theta)^{5/3}} \tag{2.15}$$

where, σ_{u}^{2} is the variance of $U(t)$ at reference height of 10 m. The derivable variable is given by

$$\theta = \frac{\omega}{\omega_{\mathrm{p}}}$$

where, ω_{p} is the peak frequency.

(b) *API (2000) spectrum*

$$\frac{\omega S_{\mathrm{u}}^{+}(\omega)}{\sigma_{\mathrm{u}}(z)^{2}} = \frac{\left(\omega/\omega_{\mathrm{p}}\right)}{\left[1+1.5\left(\omega/\omega_{\mathrm{p}}\right)\right]^{5/3}} \tag{2.16}$$

where, ω_{p} is peak frequency and σ_{z}^{2} is the variance of $U(t)$, which is not assumed as independent.

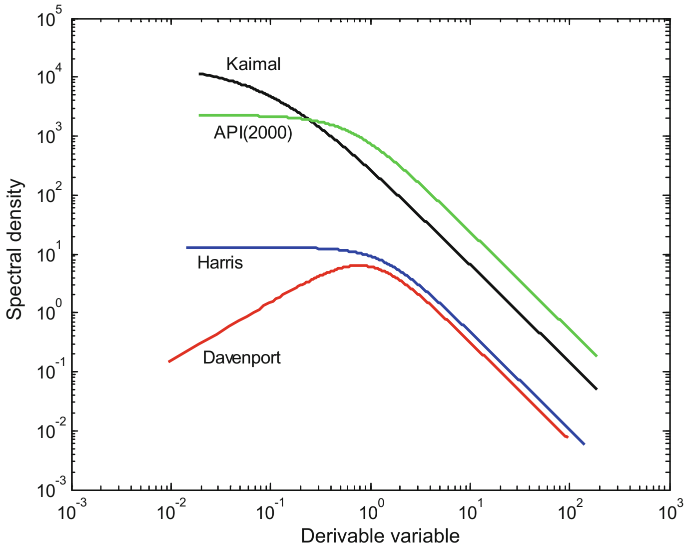

Fig. 2.1 Wind spectra

$$0.01 \le \frac{\omega_p z}{\overline{U}(z)} \le 0.1 \tag{2.17}$$

Usually, a value of 0.025 is obtained in lieu of the values computed from the above equation. Standard deviation and speed is given by

$$\sigma_u(z) = \begin{cases} 0.15\overline{U}(z)\left(\frac{Z_s}{Z}\right)^{0.125} & : Z \le Z_s \\ 0.15\overline{U}(z)\left(\frac{Z_s}{Z}\right)^{0.275} & : Z > Z_s \end{cases} \tag{2.18}$$

where, Z_s is the thickness of the surface layer, which is usually taken as 20 m. The spectral density plot showing different wind spectra for mean wind speed of 20 m/s and time period 12 s at a reference height of 10 m is given in Fig. 2.1.

2.4 Computer Code for Wind Spectra

The MATLAB program for plotting the wind spectra is given below. The variables are mean wind speed and time period.

```
%%wind spectra plot---- spectral density versus theta
%%davenport spectrum
um=20; %mean wind speed at a height of 10 m
```

```
del=0.001; %surface drag coefficient
lu=1200; %integral length for davenport spectrum in m
w=0.001:0.001:10; %frequency is the varying component
theta=(w*lu)/(2*pi*um);
a=4*((theta).^2);
b=(1+(theta.^2)).^(4/3);
x=a./b;
y=(x*del*(um^2));
su=y./w;
%%harris spectrum
um=20; %mean wind speed at a height of 10 m
del=0.001; %surface drag coefficient
lu=1800; %integral length for harris spectrum in m
w=0.001:0.001:10; %frequency is the varying component
theta1=(w*lu)/(2*pi*um);
a=4*theta1;
b=(2+(theta1.^2)).^(5/6);
x=a./b;
y=x*del*(um^2);
su1=y./w;
%%Kaimal spectrum
t=12; %time period in seconds
w=0.01:0.001:100; %frequency is the varying component
wp=(2*pi)/t; %frequency in radians per second
z=10; %reference height is 10 m
zs=20; %the surface height usually taken as 20 m
uz=(wp*z)/0.025;
if z<=zs
  sigma=0.15*uz*((zs/z)^0.125);
else
  sigma=0.15*uz*((zs/z)^0.275);
end
theta2=w./wp;
a=6.8*theta2;
b=(1+(10.2*theta2)).^(5/3);
x=a./b;
y=x.*(sigma^2);
su2=y./w;
%%API(2000) spectrum
t=12; %time period in seconds
w=0.01:0.001:100; %frequency is the varying component
wp=(2*pi)/t; %frequency in radians per second
z=10; %reference height is 10 m
zs=20; %the surface height usually taken as 20 m
uz=(wp*z)/0.025;
```

```
if z<=zs
  sigma=0.15*uz*((zs/z)^0.125);
else
  sigma=0.15*uz*((zs/z)^0.275);
end
theta3=w./wp;
b=1+(1.5*(theta3)).^(5/3);
x=theta3./b;
y=x.*(sigma^2);
su3=y./w;
loglog(theta,su,'r','linewidth',2);%Davenport Spectrum
hold on;
loglog(theta1,su1,'b:','linewidth',2);%Harris spectrum
hold on;
loglog(theta2,su2,'k-.', 'linewidth',2);%Kaimal
hold on;
loglog(theta3,su3,'c--','linewidth',2);
xlabel('Derivable variable');
ylabel('Spectral density');
title('WIND SPECTRA (Mean wind speed=20m/s, Reference Height=10m, Time
period=12s)');
```

2.5 Wave Forces

Wind-generated sea surface waves can be represented by a combination of regular waves. Regular waves of different magnitude and wave lengths from different directions are combined to represent the sea surface elevation. Water particle kinematics of regular waves is expressed by the sea surface elevation by various wave theories (Chandrasekaran and Bhattacharyya 2011).

2.6 Wave Theories

Wave theories serve to calculate the particle velocities, accelerations, and the dynamic pressure as functions of the surface elevation of the waves. For long-crested regular waves, the flow can be considered two-dimensional and are characterized by parameters such as wave height (*H*), period (*T*), and water depth (*d*), as shown in Fig. 2.2. $k(=2\pi/L)$ denotes the wave number, $\omega = 2\pi/T$ denotes the wave circular frequency and $f(=1/T)$ denotes the cyclic frequency. Different wave theories available are as follows:

- Linear or first-order or Airy theory
- Stokes fifth-order theory
- Solitary wave theory
- Cnoidal theory
- Dean's stream function theory
- Numerical theory by Chappelear

Figure 2.3 shows the chart for the selection of the most appropriate theory, based on the parameters, *H*, *T,* and *d*. For example, linear wave theory can be applied when $H/gT^2 < 0.01$ and $d/GT^2 > 0.05$, besides other ranges, as shown in the figure.

2.6.1 Airy's Wave Theory

Among all the theories, Airy's wave theory is commonly used because it assumes linearity between the kinematic quantities and the wave height, which makes the wave theory simple. Airy's theory assumes a sinusoidal wave form of wave height (*H*), which is small in comparison to the wave length (λ) and water depth (*d*) as given below

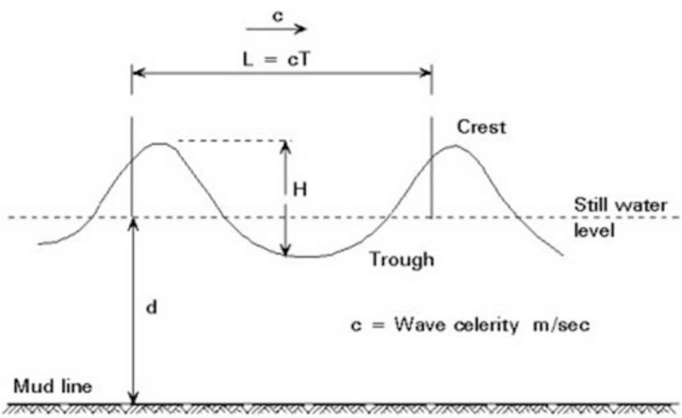

Fig. 2.2 Definition of wave parameters

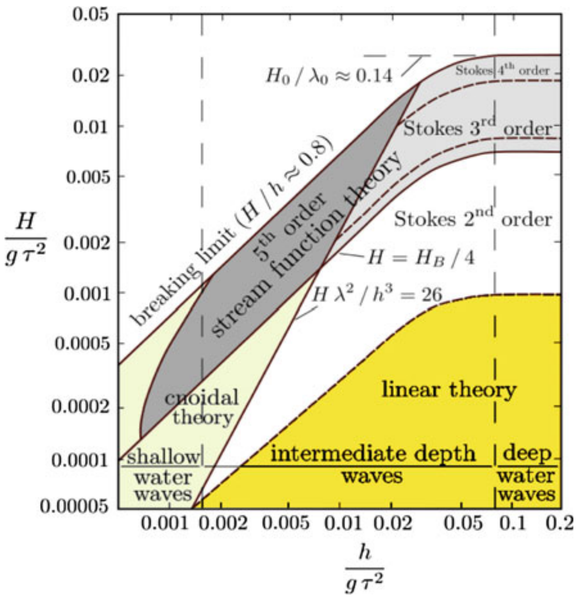

Fig. 2.3 Wave theory chart (Sarpakaya and Issacson 1981)

$$
\begin{aligned}
\eta(x,t) &= \frac{H}{2}\cos(kx-\omega t)\\
k &= \frac{2\pi}{\lambda}\\
\dot{u}(x,t) &= \frac{\omega H}{2}\frac{\cosh(ky)}{\sinh(kd)}\cos(kx-\omega t)\\
\dot{v}(x,t) &= \frac{\omega H}{2}\frac{\sinh(ky)}{\sinh(kd)}\sin(kx-\omega t)\\
\ddot{u}(x,t) &= \frac{\omega^2 H}{2}\frac{\cosh(ky)}{\sinh(kd)}\sin(kx-\omega t)\\
\ddot{v}(x,t) &= -\frac{\omega^2 H}{2}\frac{\sinh(ky)}{\sinh(kd)}\cos(kx-\omega t)
\end{aligned}
\tag{2.19}
$$

The waves are classified according to depth as shallow, intermediate, and deep-water waves depending on the ratio of the water depth to wavelength. Variations in horizontal and vertical water particle velocities for different water depth conditions are shown in Fig. 2.4.

Airy's theory is valid up to mean sea level only. However, due to the variable submergence effect, the submerged length of the members will be continuously changing. This will attract additional forces due to their variable submergence at any given time. To compute the water particle kinematics up to the actual level of submergence, stretching modifications suggested by various researchers are used.

Fig. 2.4 Variations in vertical and horizontal water particle velocities

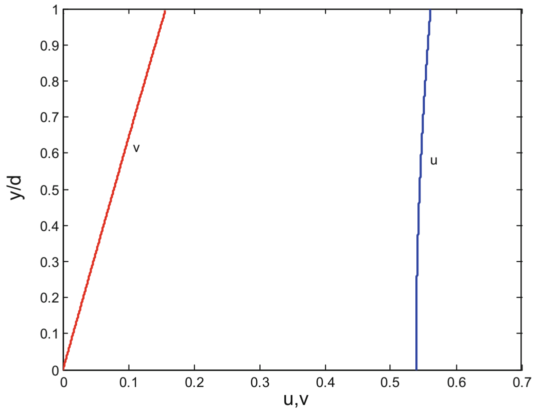

(a) Shallow water condition

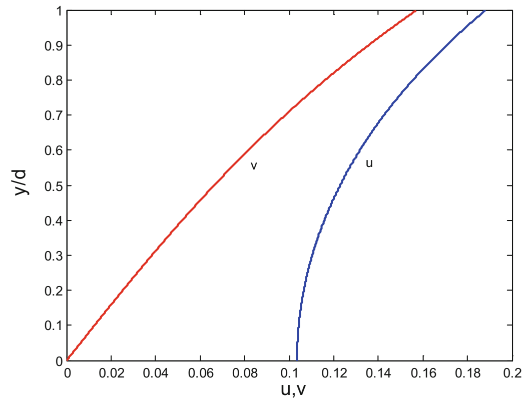

(b) Intermediate water condition

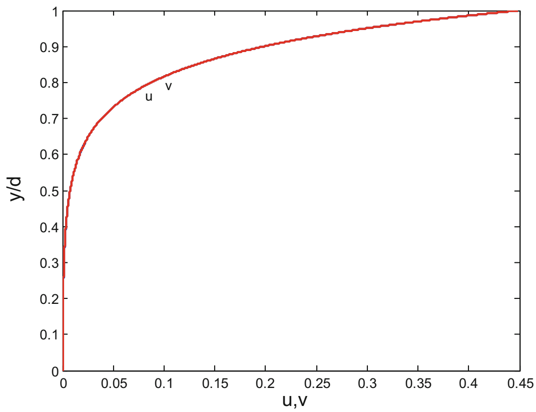

(c) Deep water condition

Wheeler suggested the following modifications in the horizontal water particle velocity and acceleration to include the actual level of submergence of the member:

$$\begin{aligned}\dot{u}(x,t) &= \frac{\omega H}{2}\frac{\cosh\left(ky\left[\frac{\mathrm{d}}{\mathrm{d}+\eta}\right]\right)}{\sinh(kd)}\cos(kx-\omega t)\\ \ddot{u}(x,t) &= \frac{\omega^2 H}{2}\frac{\cosh\left(ky\left[\frac{\mathrm{d}}{\mathrm{d}+\eta}\right]\right)}{\sinh(kd)}\sin(kx-\omega t)\end{aligned} \tag{2.20}$$

Chakrabarti suggested the modifications as given below

$$\begin{aligned}\dot{u}(x,t) &= \frac{\omega H}{2}\frac{\cosh(ky)}{\sinh(k(\mathrm{d}+\eta))}\cos(kx-\omega t)\\ \ddot{u}(x,t) &= \frac{\omega^2 H}{2}\frac{\cosh(ky)}{\sinh(k(\mathrm{d}+\eta))}\sin(kx-\omega t)\end{aligned} \tag{2.21}$$

Variations in the horizontal water particle velocity for the intermediate water depth condition, based on the modifications are shown in Fig. 2.5. As seen from the figure, horizontal water particle velocity variation increases with the increase in the wave height. The same variation is observed in deep and shallow water conditions also. At a wave height less than 1 m, the variations due to Wheeler's and Chakrabarti's modifications were found to be very small.

2.6.2 Stoke's Fifth-Order Theory

Airy's theory is the simplified theory, which is applicable only for waves of small heights. Stoke's theory extended the range covered by the Airy theory to the waves of greater steepness (Stokes 1880). The coefficients in the series involving five terms are complicated which restricts the usage of this theory widely. The Stoke's coefficients and equations are listed below

$$\begin{aligned}s &= \sinh kd\\ c &= \cosh kd\\ C_o^2 &= g\ \tanh kd\end{aligned}$$

Fig. 2.5 Horizontal water particle velocity variation in intermediate water condition

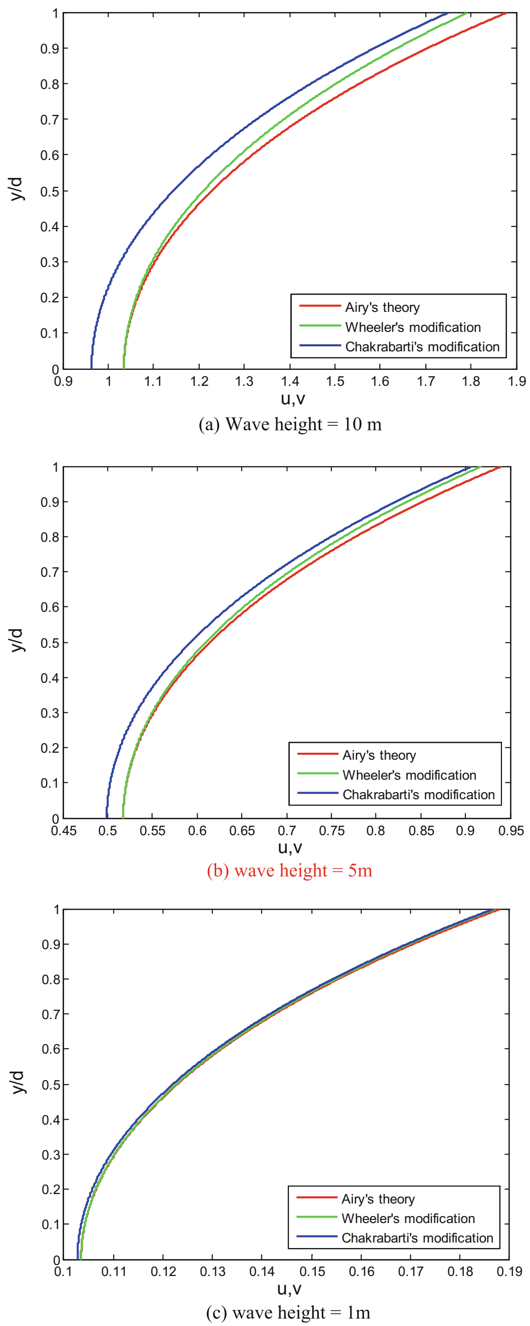

$$A_{11} = \frac{1}{s}$$
$$A_{13} = \frac{-c^2(5c^2+1)}{8s^5}$$
$$A_{15} = \frac{-\left(1184c^{10} - 1440c^8 - 1992c^6 + 2641c^4 - 249c^2 + 18\right)}{1536s^{11}}$$
$$A_{22} = \frac{3}{8s^4}$$
$$A_{24} = \frac{\left(192c^8 - 42c^6 - 312c^4 + 480c^2 - 17\right)}{768s^{10}}$$
$$A_{33} = \frac{(13-4c^2)}{64s^7}$$
$$A_{35} = \frac{\left(512c^{12} + 4224c^{10} - 6880c^8 - 12808c^6 + 16704c^4 - 315c^2 + 107\right)}{4096s^{13}(6c^2-1)}$$
$$A_{44} = \frac{\left(80c^6 - 816c^4 + 1338c^2 - 197\right)}{1536s^{10}(6c^2-1)}$$
$$A_{55} = \frac{\left(2880c^{10} - 72480c^8 + 324000c^6 - 432000c^4 + 163470c^2 - 16245\right)}{61440s^{11}(6c^2-1)(8c^4-11c^2+3)}$$

$$B_{22} = \frac{(2c^2+1)c}{4s^3}$$
$$B_{24} = \frac{c\left(272c^8 - 504c^6 - 192c^4 + 322c^2 + 21\right)}{8384}$$
$$B_{33} = \frac{3\left(8c^6+1\right)}{64s^6}$$
$$B_{35} = \frac{\left(88128c^{14} - 208224c^{12} + 70848c^{10} + 54000c^8 - 21816c^6 + 6264c^4 - 54c^2 - 81\right)}{12288s^{12}(6c^2-1)}$$
$$B_{44} = \frac{\left(764c^{10} - 448c^8 - 48c^6 + 48c^4 + 106c^2 - 21\right)c}{384s^9(6c^2-1)}$$
$$B_{55} = \frac{\left(192000c^{16} - 262720c^{14} + 83680c^{12} + 20160c^{10} - 7280c^8 + 7160c^6 - 1800c^4 - 1050c^2 + 225\right)}{12288s^{10}(6c^2-1)(8c^4-11c^2+3)}$$

$$C_1 = \frac{(8c^4 - 8c^2 + 91)}{8s^4}$$
$$C_2 = \frac{\left(3840c^{12} - 4096c^{10} + 2592c^8 - 1008c^6 + 5944c^4 - 1830c^2 + 147\right)}{512s^{10}(6c^2-1)}$$
$$C_3 = \frac{1}{4sc}$$
$$C_4 = \frac{\left(12c^8 + 36c^6 - 162c^4 + 141c^2 - 27\right)}{192cs^9}$$

The water particle velocities are given by

$$u = C\sum_{n=1}^{5} nF_n \cos n\theta \cosh nkS$$
$$w = C\sum_{n=1}^{5} nF_n \sin n\theta \sinh nkS$$

2.6.3 Wave Data

Wave data are approximately collected for 20 min every 3 h and assumed to represent the stationary sea state between the measurements. The sea state is defined by significant wave height, significant wave period, peak period, and wave direction. Data collection is done by visual investigation and instrumental observations by buoys, radars, lasers, and satellites. The sea state, in a short term, which is typically 3 h, is assumed as zero mean, ergodic Gaussian process. This can be defined completely by a wave spectrum. For North Sea, JONSWAP spectrum is recommended. For open sea conditions, Peirson-Moskowitz (PM) spectrum is recommended. In a long term, variation of sea state is slower than the short-term fluctuations. It is often approximated by a series of stationary, nonzero-mean Gaussian process, which is specified by the significant wave height (H_s) and peak wave period (T_p). Following are a few relevant spectra, applicable in the design of offshore platforms.

2.7 Wave Spectra

The wave spectrum describes the energy distribution of different frequencies of a sea state. The spectrum should be selected based on the frequency characteristics of the wave environment (Boaghe et al. 1998; Issacson and Det 1982).

(a) *PM spectrum for wave loads*

PM spectrum is a one parameter spectrum and it used for fully developed sea condition as generated by relatively moderate winds over large fetches.

$$S^{+}(\omega) = \frac{\alpha g^2}{\omega^5} \exp\left[-1.25\left(\frac{\omega}{\omega_0}\right)^{-4}\right] \tag{2.22}$$

where, α is Phillips constant $\cong$0.0081.

(b) *Modified PM spectrum (2 parameters H_s, ω_0)*

This is a two parameter spectrum which was developed to account for the wave height. This spectrum is suitable for fully developed sea condition and it is usually employed to describe the tropical storm waves generated by hurricanes. It has a greater frequency bandwidth.

$$S^{+}(\omega) = \frac{5}{16} H_s \frac{\omega_0^4}{\omega^5} \exp\left[-1.25\left(\frac{\omega}{\omega_0}\right)^{-4}\right] \tag{2.23}$$

(c) *ISSC spectrum (International Ship Structures Congress) (2 parameters H_s, $\bar{\omega}$)*

ISSC spectrum is slight modification of Bretschneider spectrum and it recommended for fully developed sea condition. This spectral equation is true only for a narrow-banded spectrum and the wave elevation follows a Gaussian distribution.

$$S^{+}(\omega) = 0.1107 H_s \frac{\omega^{-4}}{\omega^5} \exp\left[-0.4427\left(\frac{\omega}{\bar{\omega}}\right)^{-4}\right] \tag{2.24}$$

$$\bar{\omega} = \frac{M_1}{M_0}$$

where, M_1 and M_0 are spectral moments.

(d) *JONSWAP (Joint North Sea Wave Project) spectrum (Five parameters H_s, ω_{0o}, γ, τ_a, τ_b).*

JONSWAP spectrum is a modified form of PM spectrum and it is recommended for use in the reliability analysis. This spectrum is applicable only for limited fetch and it is used to describe the winter storm waves of the North Sea.

$$S^{+}(\omega) = \frac{\bar{\alpha} g^2}{\omega^5} \exp\left[-1.25\left(\frac{\omega}{\omega_0}\right)^{-4}\right] \gamma^{a(\omega)} \tag{2.25}$$

where, γ is the peakedness parameter. The value of 3.3 yields a mean spectrum for a specified wind speed and a given fetch length. The variation of the peakedness parameter depends upon the duration of the wind and stage of growth and decay of the storm. This value follows a normal probability distribution.

$$a(\omega) = \exp\left[-\frac{(\omega - \omega_0)^2}{2\bar{\sigma}^2 \omega_0^2}\right] \tag{2.26}$$

where, $\bar{\sigma}$ is spectral width parameter or shape parameter and is given by

$$\bar{\sigma}_a = 0.07, \omega \leq \omega_0 \tag{2.27}$$

$$\bar{\sigma}_b = 0.09, \omega > \omega_0 \tag{2.28}$$

The modified Phillips constant is given by

$$\bar{\alpha} = 3.25 \times 10^{-3} H_s^2 \omega_0^4 [1 - 0.287 \ln(\gamma)] \tag{2.29}$$

$$\gamma = 5 \quad \text{for} \quad \frac{T_\text{p}}{\sqrt{H_\text{s}}} \leq 3.6 \tag{2.30}$$

$$= \exp\left[5.75 - 1.15 \frac{T_\text{p}}{\sqrt{H_\text{s}}}\right] \quad \text{for} \quad \frac{T_\text{p}}{\sqrt{H_\text{s}}} > 3.6 \tag{2.31}$$

$$H_\text{s} = 4\sqrt{m_0} \tag{2.32}$$

where, γ varies from 1 to 7.

The wave spectra plot, as shown in Fig. 2.6 illustrates comparison for significant mean wind speed 20 m/s, wave height 5 m, and time period 10 s. It is seen from the figure that Modified PM spectrum and ISSC spectrum have the same spectral distribution while JONSWAP spectrum shows the high energy peak.

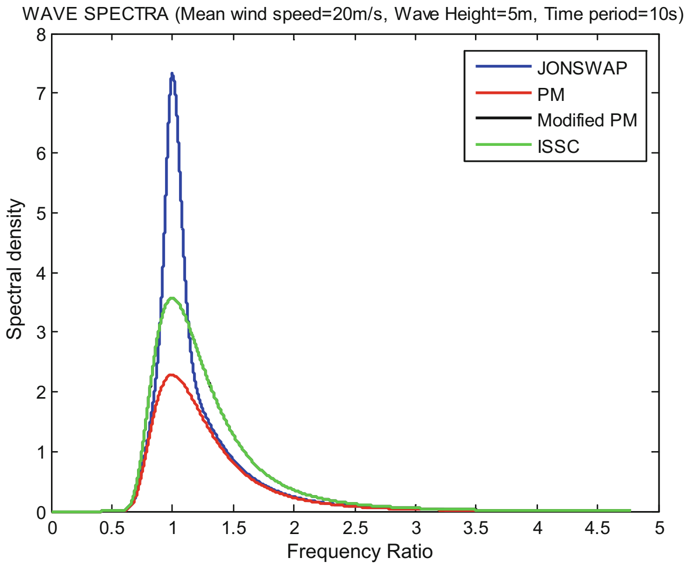

Fig. 2.6 Comparison of wave spectra

2.7.1 Computer Code for Wave Spectra Plots

The MATLAB program for the wave spectra plot is given below. The variables are mean wind speed, significant wave height and time period.

```
%%WAVE SPECTRA plot ---- spectral density versus frequency ratio
%%Jonswap spectrum
hs=5; %wave height in m
t=10; %time period in seconds
v=3; %peakedness factor chosen between 1 to 7
g=9.81; %gravitational constant
w=0:0.000001:3; %frequency is the varying component
n=length(w);
wo=(2*pi)/t;
alpha=3.25*(10^-3)*(hs^2)*(wo^4)*(1-(0.287*(log(v))));
for i=1:n
if w(i)<=wo
  sigma(i)=0.07;%spectral width parameter
else
  sigma(i)=0.09;
end
x(i)=-((w(i)-wo)^2)/(2*(sigma(i)^2)*((wo)^2));
y(i)=-1.25*((w(i)/wo)^(-4));
aw(i)=exp(x(i));
z(i)=exp(y(i))*(v^aw(i))*alpha*(g^2);
s(i)=z(i)/(w(i)^5);
p(i)=w(i)/wo;
i=i+1;
end
%%PM spectrum
hs=5; %wave height in m
t=10; %time period in seconds
g=9.81; %gravitational constant
v=20; %mean wind speed in m/s
wo=(2*pi)/t;
w=0:0.0001:3; %frequency is the varying component
n=length(w);
for i=1:n
x(i)=-1.25*((w(i)/wo)^(-4));
a(i)=exp(x(i));
b(i)=1/((w(i))^5);
s1(i)=0.0081*a(i)*b(i)*(g)^2;
p1(i)=w(i)/wo;
i=i+1;
```

```
end
%%Modified PM spectrum
hs=5; %wave height in m
t=10; %time period in seconds
wo=(2*pi)/t;
w=0:0.0001:3; %frequency is the varying component
n=length(w);
for i=1:n
y(i)=(-1.25)*((w(i)/wo)^(-4));
a(i)=exp(y(i));
b(i)=(wo^4)/((w(i))^5);
s2(i)=0.3125*((hs^2)*a(i)*b(i));
p2(i)=w(i)/wo;
i=i+1;
end
%%ISSC spectrum
hs=5; %wave height in m
t=10; %time period in seconds
wo=(2*pi)/t;
w=0:0.0001:3; %frequency is the varying component
n=length(w);
for i=1:n
y(i)=-1.2489*((w(i)/wo)^(-4));
a(i)=exp(y(i));
b(i)=(wo^4)/((w(i))^5);
s3(i)=0.3123*((hs^2)*a(i)*b(i));
p3(i)=w(i)/wo;
i=i+1;
end
plot(p,s,'k'); %jonswap spectrum
hold on;
plot(p1,s1,'r');%Modified PM spectrum
hold on;
plot(p2,s2,'b'); %Bretschneider spectrum
hold on;
plot(p3,s3,'g'); %ISSC spectrum
xlabel('Frequency Ratio');
ylabel('Spectral density');
title
('WAVE SPECTRA (Mean wind speed=20m/s, Wave Height=5m, Time period=10s)');
```

2.8 Wave Force on Cylinders

Main force components, rising from the wave loads are grouped as follows: (i) *Froude-Krylov force*, which is caused by the pressure effects due to the undisturbed incident waves; (ii) *diffraction force*, which is caused by the pressure effects due to the presence of the structure in the fluid-flow domain; (iii) *hydrodynamic added mass and potential damping forces*, which is caused by the pressure effects due to the motion of the structural components in ideal fluid; and (iv) *viscous drag force*, which is caused by the pressure effects due to the relative velocity between the water particle and the structural component. For slender structures, *Froude-Krylov force and diffraction forces* are idealized by a single inertia term. Velocity and acceleration do not differ significantly from the values of the cylinder axis when $D/\lambda < 0.2$. When the waves act on the slender structures, the structure oscillates, which will set up waves radiating away from it. Reaction forces are then set up in the fluid, which will be proportional to the acceleration and velocity of the structure. Reaction force proportional to the acceleration of the structure will result in an added mass term, contributing to the inertia force. Reaction force proportional to the velocity results in the potential damping force. If the structure is compliant, the added mass forces associated with the relative acceleration between the fluid particles and the structures are included. Drag force will be computed by replacing the water particle velocity with the relative velocity term. The total force acting normal to the axis of the member is given by

$$\begin{aligned} q_n &= \rho \mathrm{d}V.a_n + (C_m - 1)\rho \mathrm{d}V(a_n - \ddot{x}_n) + \frac{1}{2}\rho C_d \mathrm{d}A(v_n - \dot{x}_n)|v_n - \dot{x}_n| \\ &= C_m \rho \mathrm{d}V.a_n - (C_m - 1)\rho \mathrm{d}V\ddot{x}_n + \frac{1}{2}\rho C_d \mathrm{d}A(v_n - \dot{x}_n)|v_n - \dot{x}_n| \end{aligned} \quad (2.33)$$

where, ρ is density of fluid, (C_d, C_m) are the drag and inertia coefficients, (v_n, a_n) are velocity and acceleration of the water particle normal to the axis of the member, $\dot{x}, \ddot{x}$ are the velocity and acceleration of the structure, and (dA, dV) are exposed area and displaced volume of water per unit length, respectively.

The above equation has two main issues: first, the relative motion formulation is valid only if the structure motion is of large amplitude; second, the relative velocity formation of the drag produces both excitation and damping forces. In the above equation, the most critical aspect is the evaluation of the drag and inertia coefficients, which is dependent on flow conditions, Keulegan–Carpenter number and Reynolds number. The recommended value of drag coefficient is 0.6–1.2, while that of the inertia coefficient is 1.2–2.0, as seen in the literature (APR RP 2A). As in the case of bottom-supported structures (gravity platforms), when the diameter of the member is very large, incident waves are disturbed by the presence of the structure.

In such cases, viscous force becomes less significant due to the smaller values of the ratio of wave height to member diameter ($H/D \ll 1$). In such cases, the above equations cannot be applied; it is recommended that the analyzer should use numerical methods to determine the forces on the members. The variation of forces at the mean sea level with respect to phase angle is shown in Fig. 2.7, where a wave height of 5 m, period of 10 s, water depth of 50 m and diameter of the member of 1 m is used for the plot.

The variation of the total force with respect to depth is shown in Fig. 2.8. Force variation shown in the plot corresponds to the maximum phase angle.

Offshore structures have large plane area. Larger topside is required for accommodating the equipment layout as discussed in the previous chapter. As the deck will be supported on a few column members in order to reduce the interference of the waves by the presence of column members, their spacing plays an important role. For a large spacing of *c*/*c* distance of column members, there can be cancelation of forces. Let us consider an example of the tension leg platform (TLP). For a typical size of topside of 90 m × 90 m, resting on four columns, phase angle (θ) is given by the following relationship:

$$\theta = \frac{2\pi\Delta x}{\lambda} \tag{2.34}$$

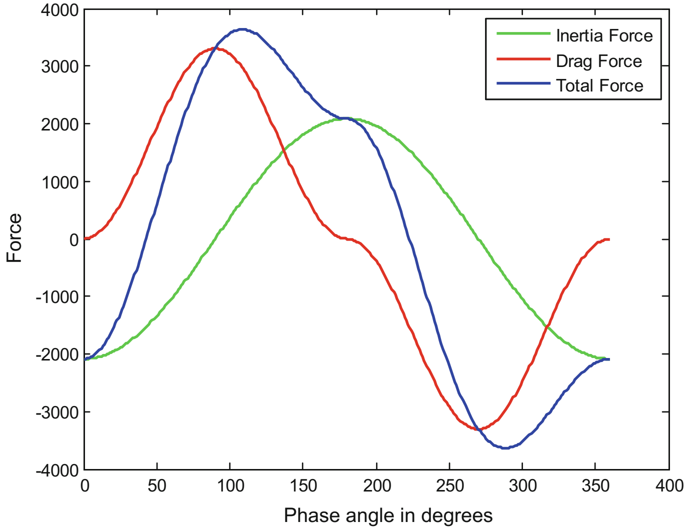

Fig. 2.7 Force variation with respect to phase angle

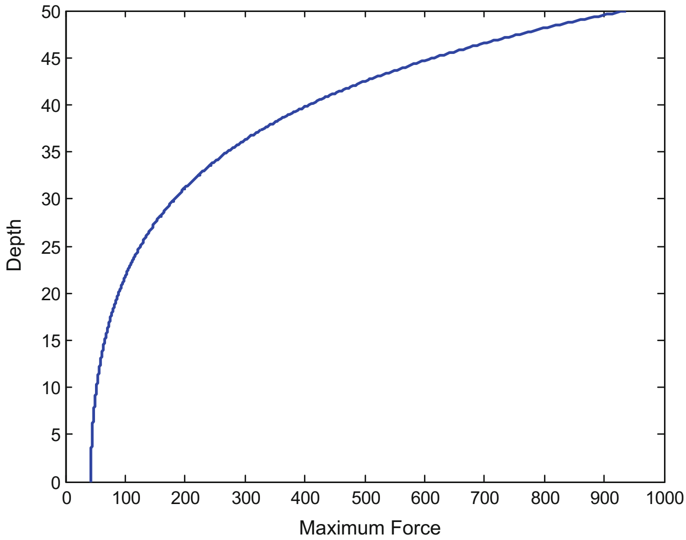

Fig. 2.8 Force variation with respect to depth

where, Δx the is *c*/*c* distance between the column members (leg spacing) and λ is the wave length. For the spacing between the columns of 90 m and wave period of 10 s, the phase angle will be 1.2π, which can cause cancelation of forces on members. It is important to note that the spacing of the members are chosen in such a manner that the force cancelation effects at the dominant wave frequencies are expected to have close to the natural frequency of the platform. The forces on a submerged structure in waves appear from the pressure distribution on its surface. For a small structure, Morison equation is valid because the flow structure is complex. However, for large structures (relative to the wavelength) the flow remains essentially attached to the surface. It is therefore easier to compute this pressure field. If the computation of the scattered wave potential is waived and its effect is incorporated by a force coefficient, then this force is called the *Froude-Krylov* force. Thus, the calculation of the force is performed assuming that the structure does not distort the wave field in its vicinity. The force is computed by a pressure area method using the incident wave pressure that is acting on the submerged surface of the structure. Then a force coefficient is used to account for the wave diffraction.

For a few basic shapes of the structural forms, a closed form expression may be obtained by the Froude-Krylov theory: (i) horizontal cylinder, (ii) horizontal half-cylinder, (iii) vertical cylinder, (iv) sphere, (v) hemisphere and (vi) rectangular barge.

(a) Force on a horizontal cylinder is given by

$$f_{\mathrm{H}} = r\ell \int_{0}^{2\pi} p \cos\theta \mathrm{d}\theta \tag{2.35}$$

(b) Force on a vertical cylinder:

Consider a vertical cylinder placed on the ocean bottom and extended above the still water level, as shown in Fig. 2.9

Velocity potential is given by

$$\varphi = \frac{gH}{2\omega} \frac{\cosh(ks)}{\cos h(kd)} \sinh(kx - \omega t) \tag{2.36}$$

Dynamic pressure is given by

$$\begin{aligned} p &= \rho \frac{\partial \varphi}{\partial t} \\ &= \rho g \frac{H}{2} \frac{\cosh(ks)}{\cosh(kd)} \cos(kx - \omega t) \end{aligned} \tag{2.37}$$

Variation of dynamic pressure at a depth of 10 m with significant wave height 5 m and the total water depth is 20 m is shown in Fig. 2.10.

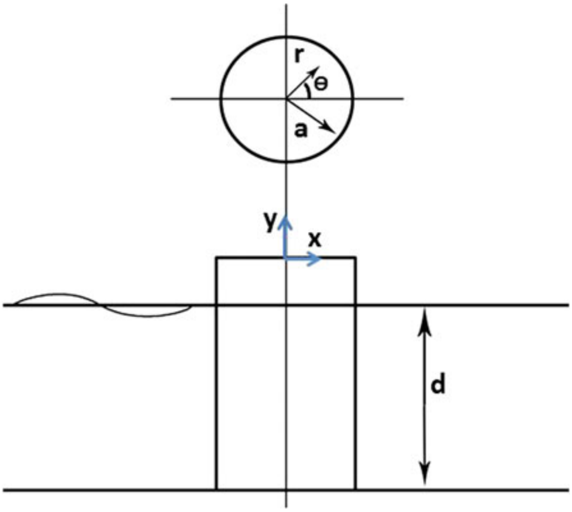

Fig. 2.9 Bottom-supported cylinder

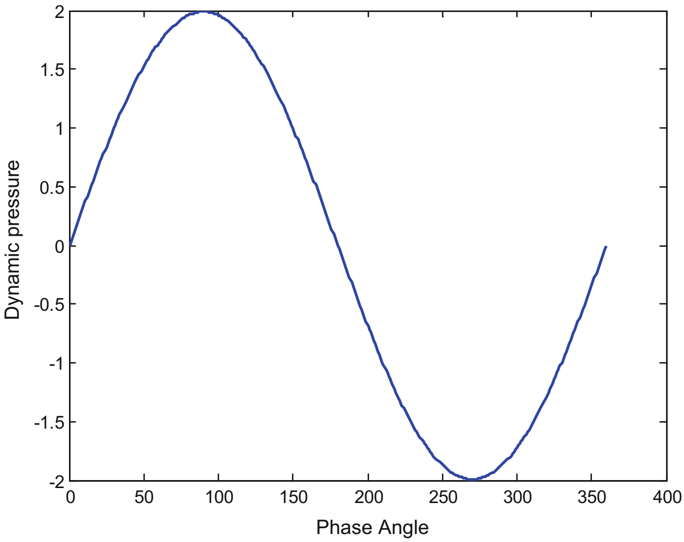

Fig. 2.10 Dynamic pressure variation

Horizontal force per unit length is given by

$$\begin{aligned} f_x &= \rho \int_0^{2\pi} \int_{-d}^{0} \frac{\partial \varphi_0}{\partial t} a \cos \theta \mathrm{d}\theta \mathrm{d}\ell \\ f_x &= \frac{\rho g a H}{2\cosh(kd)} \int_{-d}^{0} \cos h(ks) ds \int_0^{2\pi} \cos[ka\cos\theta - \omega t] \cos\theta \mathrm{d}\theta \end{aligned} \tag{2.38}$$

This reduces the following form, which accounts for diffraction effect:

$$f_x = C_H \frac{\pi \rho g H a}{k} J_1(ka) \tanh(kd) \sin \omega t \tag{2.39}$$

The above method of computing the forces by the incident wave alone is known as Froude-Krylov theory. It does not give the correct value of the force, as the phase value is accounted for in the equation. It is due to this fact a force coefficient is used in the expression as a multiplier. For a vertical cylinder, the horizontal force coefficient is taken as 2; for small values of *ka*; the value changes as *ka* increases. Table 2.1 shows the equations for forces using Froude-Krylov theory for different geometric shapes of members. Numerical values of C_1–C_4 depend on the diffraction

Table 2.1 Forces on members of different geometric shapes using Froude-Krylov theory

Basic shape	Horizontal force	C_H	Vertical force	C_V	K_a range
Horizontal cylinder	$C_H \rho V \dot{u}_0$	2.0	$C_V \rho V \dot{v}_0$	2.0	0–1.0
Horizontal half-cylinder	$C_H \rho V [\dot{u}_0 + C_1 \omega v_0]$	2.0	$C_V \rho V [\dot{v}_0 + C_2 \omega u_0]$	1.1	0–1.0
Vertical cylinder	$C_H \rho V \frac{2J_1(ka)}{ka} \frac{\sinh\left[\frac{k\ell_1}{2}\right]}{\left[\frac{k\ell_1}{2}\right]} \dot{u}_0$	2.0	–	–	–
Rectangular block	$C_H \rho V \frac{\sinh\left[\frac{k\ell_3}{2}\right]}{\left[\frac{k\ell_3}{2}\right]} \frac{\sinh\left[\frac{k\ell_1}{2}\right]}{\left[\frac{k\ell_1}{2}\right]} \dot{u}_0$	1.5	$C_V \rho V \frac{\sinh\left[\frac{k\ell_3}{2}\right]}{\left[\frac{k\ell_3}{2}\right]} \frac{\sinh\left[\frac{k\ell_1}{2}\right]}{\left[\frac{k\ell_1}{2}\right]} \dot{v}_0$	6.0	0–5.0
Hemi sphere	$C_H \rho V [\dot{u}_0 + C_3 \omega v_0]$	1.5	$C_V \rho V [\dot{v}_0 + C_4 \omega u_0]$	1.1	0–0.8
Sphere	$C_H \rho V \dot{u}_0$	1.5	$C_V \rho V \dot{v}_0$	1.1	0–1.75

Where V = submerged volume of the structure; C_H and C_V are force coefficients in the horizontal and vertical directions, respectively; subscript zero indicates that the amplitude of the water particle velocity or acceleration is computed at the center of the geometric shape; l_1 and l_3 are the length and underwater depth of the rectangular block, respectively

Table 2.2 Numerical values of C_1–C_4

ka	C_1	C_2	C_3	C_4
0.1	0.037	15.019	0.042	12.754
0.2	0.075	7.537	0.085	6.409
0.3	0.112	5.056	0.127	4.308
0.4	0.140	3.825	0.169	3.268
0.5	0.186	3.093	0.210	2.652
0.6	0.223	2.612	0.252	2.249
0.7	0.259	2.273	0.292	1.966
0.8	0.295	2.024	0.332	1.760
0.9	0.330	1.834	0.372	1.603
1.0	0.365	1.685	0.411	1.482
1.5	0.529	1.273	0.591	1.156
2.0	0.673	1.105	0.745	1.034
2.5	0.792	1.031	0.867	0.989
3.0	0.886	0.999	0.957	0.977
3.5	0.955	0.989	1.015	0.978
4.0	1.000	0.087	1.945	0.985

parameter ka and are given Table 2.2. The forces in Table 2.1 are given in terms of the water particle acceleration and velocity at the center of the structure wherever possible. The force coefficients shown are applicable over a small range of diffraction parameter. If the values of ka are much different from the range given in the table, values of the force coefficients are to be used with caution.

2.9 Current Forces

The presence of current in water produces the following distinct effects: Current velocity should be added vectorially to the horizontal water particle velocity before computing the drag force, because drag force depends on the square of the water particle velocity. Current decreases slowly with the increase in depth, but even a small magnitude of current velocity can cause significant drag force. The opposing current will increase the force on the member and the superposed current will decrease the total force. The effect of current on the variation of total force with respect to phase angle is shown in Fig. 2.11.

This effect is insignificant and generally neglected. Current makes the structure itself to generate waves, which in turn creates diffraction forces. However, these values are negligible for realistic value of current acting on the normal-sized members. The presence of current is alternatively accounted by increasing the wave height to 10–15% and neglect the presence of current per se.

2.10 Earthquake Loads

Offshore platforms, which do not have stiff connection with the seabed are indirectly influenced by earthquakes; those which are bottom-supported are affected by earthquakes directly. Compliant structures that are position-restrained by tethers will be subjected to dynamic tether tension variations under the presence of

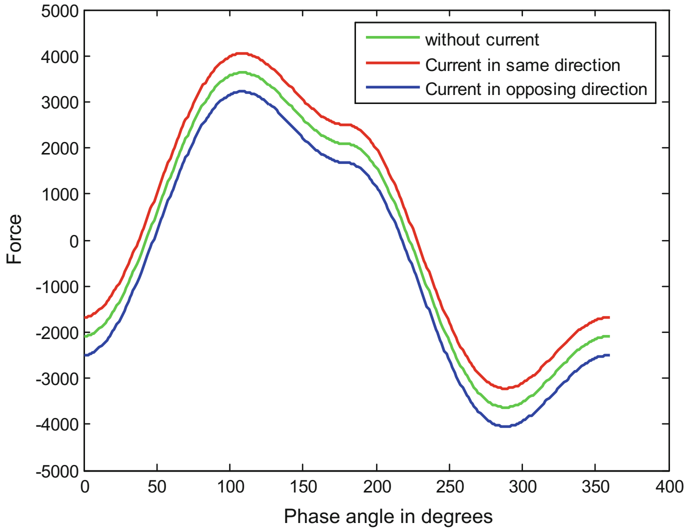

Fig. 2.11 Variation of the total force due to current

earthquake forces, which in turn shall affect the response of the platform under lateral loads. Earthquakes give rise to the horizontal and vertical motions for a typical duration of 15–30 s. Earthquake acceleration exhibits random characteristics due to (i) the nature of the mechanism causing earthquakes; (ii) wave propagation; (iii) reflection; and (iv) deflection. Earthquakes can result in inertia forces due to the acceleration and damping forces due to the motion of the water particles. In case of the analysis of compliant structures like TLPs, earthquake forces are handled in an indirect manner. Water waves generated due to the ground motion are neglected. Stiffness of TLP tether is modeled as axial tension members; slackening of tethers is neglected. The dynamic tether tension variation, caused by the horizontal motion of the earthquakes, is used to update the stiffness matrix of the TLP using the following equation (Chandrasekaran and Gaurav 2008):

$$\Delta T = \frac{AE}{\ell}\left[x(t) - x_g(t)\right] \tag{2.40}$$

where, $x(t)$ is the instantaneous response vector of TLP and $x_g(t)$ is the ground displacement vector, which is given by:

$$x_g(t) = \begin{Bmatrix} x_{1g}(t) \\ 0 \\ x_{3g}(t) \\ 0 \\ 0 \\ 0 \end{Bmatrix} \tag{2.41}$$

where, x_{1g}, x_{3g} is the horizontal and vertical ground displacements, respectively. Ground motions can be generated using Kanai-Tajimi ground acceleration spectrum (K-T spectrum), which is given by

$$\begin{aligned} S_{\ddot{x}_g\ddot{x}_g}(\omega) &= \left[\frac{\omega_g^4 + 4\xi_g^2\omega_g^2\omega^2}{\left(\omega_g^2 - \omega^2\right)^2 + 4\xi_g^2\omega_g^2\omega^2}\right] S_0 \\ S_0 &= \frac{2\xi_g\sigma_g^2}{\pi\omega_g(1 + 4\xi_g^2)} \end{aligned} \tag{2.42}$$

where, S_0 is the intensity of earthquake, ω_g is the natural frequency of the ground, ξ_g is the damping of the ground and σ_g^2 is the variance of the ground acceleration. These are the three parameters on which K-T spectrum depends on, which need to be chosen for any analytical studies on TLP under seismic action. The above three parameters should be estimated from the representative earthquake records by established estimation processes (Chandrasekaran et al. 2006a, b). For example, an earthquake occurred in GoM, approximately at 250 miles WSW of Anna Maria, Florida on 10 September 2006 at 14:56:07 (coordinated universal time). The signal

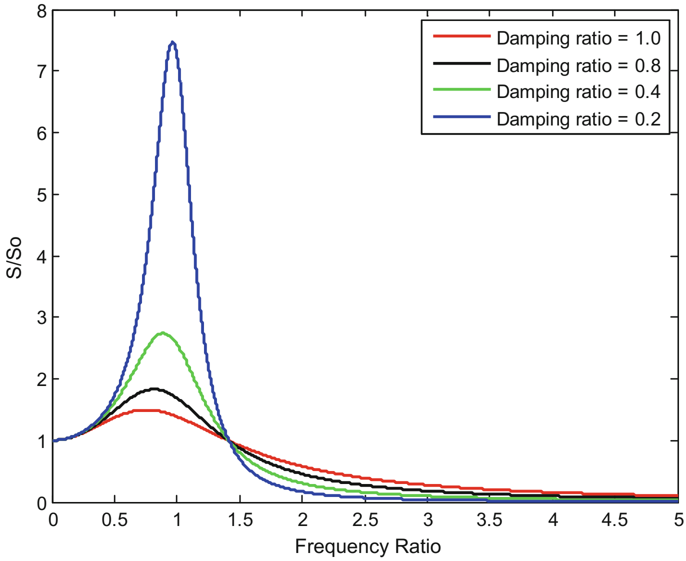

Fig. 2.12 Kanai-Tajimi ground acceleration spectrum

was epicentered 26.34N, 86.57W. Incidentally MARS TLP was operating in the Mississippi Canyon Block, which is also located in GoM. The three parameters S_0, ω_g and ξ_g are chosen such that the real earthquake is simulated for analysis purposes (Chandrasekaran and Gaurav 2008). Studies showed that the dynamic tether tension variations caused by the earthquake forces are in the order of about 65% more than that of the normal values. Even structures with rigid degrees of freedom like heave are excited, which may result in the loss of functionality of the platform. The ground acceleration spectrum is shown in Fig. 2.12. The curves are plotted for different damping ratios. It is seen from the figure that amplitude of the spectral density function tends to decrease with the increase in damping ratio.

2.11 Ice and Snow Loads

Ice loads are dominant in offshore structures in the Arctic regions. Prediction of ice loads is associated with a significant degree of uncertainty, as there are various ice conditions that exist in the service life of an offshore platform. They are level ice, broken ice, ice ridges, and icebergs. Offshore structures show different types of failure under ice loads namely creep, cracking, buckling, spalling, and crushing. Ice loads exhibit random variations in both space and time. They are classified into: (i) total or global loads and (ii) local loads or pressure. Global loads affect the overall motion and stability of the platform, while local loads affect the members at connections. In the level ice condition, frequency of interaction between the structure and ice is important; number of interactions per unit time is important to quantify the ice loads on offshore platforms. Total ice force can result in a periodic loading and can cause dynamic amplification in flexible/slender structures. Current codes include equations for the extreme static ice loads, which depend on the geometric shape of the structure. Studies show that ice loads in a conical structure are lesser than that of the cylindrical structure. This is because a well-designed cone shape can change the ice-failure mode from crushing to bending. Estimating (predicting) ice forces on offshore platforms has a lot of uncertainties. Ice forces often control the design of the platform in operational conditions, in particular. The design ice loads use varying factors for level ice, first-year ridge ice and multi-year ridge ice; the factored values are 2, 5, and 7, respectively.

There are four approaches for addressing ice forces on offshore platforms: (a) experimental studies on scaled models; (b) numerical studies; (c) field studies; and (d) data mining. Experimental studies use scaling laws to determine the ice loads and ice-structure interaction. This method claims many advantages due to the capability of testing many types of structural shapes in large testing facilities. However, such tests are expensive apart from a strong disagreement of the model ice not being accurately scaled as of the sea ice. As the ice failure is dependent on the geometric shape significantly, ice-failure behavior cannot be accurately studied. This may result in over-prediction of ice loads. Numerical modeling uses high-end software to model ice forces for different interaction scenarios, which makes it very cost-effective and instructive. However, limited validation of results with that of the experiments is reported in the literature. The more practical way to estimate ice loads is from data mining. Previous platforms can be visited to determine the ice loads through field measurements. This will give a real picture of the ice loads. In the frequency domain approach, excitation caused by ice loads is modeled as sinusoidal pseudo-excitation, and the response is characterized by the transfer function. Ice force spectrum on a narrow conical structure is given by

$$S^{+}(f) = \frac{A\overline{F}_0^2\overline{T}^{(-\delta)}}{f^{\gamma}} \exp\left[-\frac{B}{\overline{T}^{(\alpha)} f^{\beta}}\right] \tag{2.43}$$

where, A (=10), B (=5.47) are constants; $\overline{F}_0$ is the force amplitude on the structure; $\overline{T} = L_b/v$ is the period of ice; L_b is ice-breaking length, which is typically 4–10 times of thickness of ice; v is the velocity; $\alpha, \beta, \gamma, \delta$ are constants whose values are typically 0.64, 0.64, 3.5, and 2.5, respectively. Force amplitude on the structure is given by

$$\overline{F}_0 = C\sigma_f h^2 \left(\frac{D}{L_c}\right)^{0.34} \tag{2.44}$$

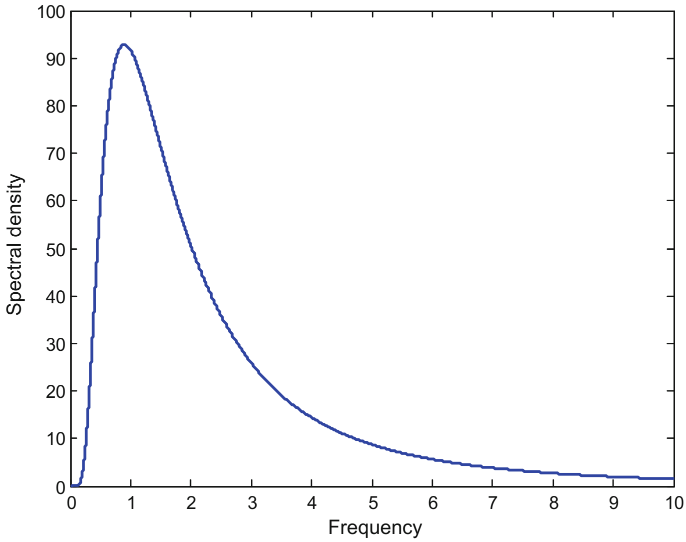

Fig. 2.13 Ice spectrum for Bohai Gulf region

where C is the constant (usually taken as 3.4); σ_f is bending strength of ice (0.7 MPa); h is the ice thickness; D is the diameter of the ice cone and L_c is the characteristic length of ice, which is given by the following equation:

$$L_c = \left[\frac{Eh^3}{12g\rho_w}\right]^{0.25} \tag{2.45}$$

where, E is Young's modulus of ice (=0.5 GPa) and ρ_w is density of water. As a sample application, spectral density plot for Bohai Gulf region is shown in Fig. 2.13. The spectrum is plotted with the variables in the above equations for the ice characteristics in the Bohai Gulf region. The variables chosen were ice thickness, velocity of ice cap and the diameter of the ice core.

2.12 Marine Growth

Marine growth or bio-fouling is the ubiquitous attachments of soft and hard bio-particles on the surface of a submerged structure. It ranges from seaweeds to hard-shelled barnacles. Its growth on the surface of the structure increases its diameter and affects its roughness. Its main effect is to increase the wave forces on the members by increasing not only exposed areas and volumes, but also the drag coefficient due to higher surface roughness. In addition, it increases the unit mass of the member, resulting in higher gravity loads and in lower member frequencies.

Depending upon the geographic location, the thickness of marine growth can reach 0.3 m or more. It is accounted for in the design through appropriate increases in the diameters and masses of the submerged members.

2.13 Mass

Mass is contributed by the structural mass and hydrodynamic added mass of the structure. For a slender structure, mass of the displaced volume of the structure will be significant and should be considered in the analysis. Added mass depends on the submerged volume of the platform, which also varies with respect to period of vibration. This is due to the variation in buoyancy, which in turn changes the tether tension variation that affects the natural frequency of motion. Based on the equipment layout plan and the chosen structural form, one can compute the mass of the platform readily. It is also important to establish the fact that a desired proportion between center of buoyancy and center of mass is maintained to ensure stability under free-floating conditions. This is important to enable smooth construction process in case of floating.

2.14 Damping

For steel offshore structures, structural damping is usually considered to vary from 0.2 to 0.5% of that of the critical damping (Adams and Baltrop 1991). For concrete structures, it can be of the order 0.5–1.5%. Hydrodynamic damping originates from the radiation damping and viscous damping effects. Radiation damping is determined using potential theory. It exhibits a strong dependence on frequency and submergence effects. Literature shows that the drag damping is lower for structures with large diameter column members ($\sim 0.1\%$). Damping ratio for offshore structures (wet structures), including the effects of added mass, can be expressed as a ratio of that of the dry structures, as given below

$$\xi_{\text{wet}} = \xi_{\text{wet}} \frac{(m^*_{\text{dry}})(\omega^*_{\text{dry}})}{(m^*_{\text{wet}})\,(\omega^*_{\text{wet}})} \tag{2.46}$$

where, m^*, ω^* are generalized mass and frequency, respectively (Naess and Moan 2013). Literature shows that the total damping ratio is about 2% for the first three modes of bottom-supported structures.

2.15 Dead Load

Dead load is the weight of the overall platform in air, which includes piling, superstructure, jacket, stiffeners, piping, conductors, corrosion anodes, deck, railing, grout, and other appurtenances. Dead load excludes the following: weight of the drilling equipment placed on the platform including the derrick, draw works, mud pumps, mud tanks, etc.; weight of production or treatment equipment located on the platform including separators, compressors, piping manifolds and storage tanks; weight of drilling supplies that cause variable loads during drilling such as drilling mud, water, fuel, casing, etc.; weight of treatment supplies employed during production such as fluid in the separator, storage in the tanks; drilling load, which is approximate combination of derrick load, pipe storage, rotary table load, etc.

2.16 Live Load

Live loads are acting in addition to the equipment loads. They include load caused by impacts of vessels and boats on the platform. Dynamic amplification factor is applied to such loads to compute the enhanced live loads. Live loads are generally designated as factor times of the applied static load. These factors are assigned by the designer depending on the type of platform. Table 2.3 gives the live load factors that are used in the platform design.

2.17 Impact Load

For structural components which experience impact under live loads, the stipulated live loads in Table 2.3 should be increased by an impact factor, as given in Table 2.4. Deck floor loads can be taken as 11.95 kN/m^2 in the drilling rig area, 71.85 kN/m^2 in the derrick area and 47.9 kN/m^2 for pipe racks, power plants and living and accommodation areas.

Table 2.3 Typical live load values used in platform design (Graff 1981a, b)

Description	Uniform load on decks (kN/m^2)	Concentrated load on deck	Concentrated load on beams
Walkway, stair	4.79	4.38 kN/m^2	4.45 kN/m^2
Areas > 40 m^2	3.11	–	–
Areas for light use	11.9	10.95 kN/m^2	267 kN

Table 2.4 Impact factor for live loads

Structural item	Load direction	
	Horizontal	Vertical
Rated load in craned	20%	100%
Drilling hook loads	–	–
Supports of light machinery	–	20%
Supports of rotating machinery	50%	50%
Boat landings (kN)	890	890

2.18 General Design Requirements

Design methodology of offshore platforms differs with different types of offshore structures. For example, vertical deformation will be lesser in case of bottom-supported structures like jacket platform, GBS, etc. Such platforms are highly rigid and tend to attract more forces. Hence the design criteria should be to limit the stresses in the members. Displacement of the members under the applied loads will be insignificant. On the contrary, compliant structures are more flexible, as they all displaced more under wave action. They also create more disturbances in the waves. Hence the design criteria will be to control displacement instead of limiting the stresses in the members. Orientation of the platform is another important aspect in the design. Preferred orientation is that members are oriented to have less projected area to the encountered wave direction. This induces lesser response on the members. Predominant wave direction for the chosen site is made available to the designer based on which the platform orientation is decided (Chandrasekaran and Bhattacharyya 2011). Following are the list of data required for the design of offshore structures:

- Land topographical survey of sufficient area covering the chosen site for platform installation
- Hydrographical survey of the proposed location (hydrographic charts are used for this purpose)
- Information regarding silting at the site
- Wind rose diagram showing information on wind velocities, duration, predominant direction round the year
- Cyclonic tracking data showing details of the past cyclonic storm such that wind velocities, direction, peak velocity period, etc., are indicated
- Oceanographic data including general tide data, tide table, wave data, local current, seabed characteristics, temperature, rainfall, and humidity
- Seismicity level and values of acceleration
- Structural data of existing similar structures, preferably in the close vicinity
- Soil investigation report

2.18.1 Steel Structures

The analysis of an offshore structure is an extensive task, embracing consideration of the different stages, i.e., execution, installation, and in-service stages, during its life. Many disciplines such as structural, geotechnical, naval architecture, and metallurgy are involved. The analytical models used in offshore engineering are in some respects similar to those adopted for other types of steel structures. Only the salient features of offshore models are presented here. The same model is used throughout the analysis with only minor adjustments to suit the specific conditions, e.g., at supports in particular, relating to each analysis. Stick models (beam elements assembled in frames) are used extensively for tubular structures (jackets, bridges, flare booms) and lattice trusses (modules, decks). Each member is (normally) rigidly fixed at its ends to other elements in the model. If more accuracy is required, particularly for the assessment of natural vibration modes, local flexibility of the connections may be represented by a joint stiffness matrix. In addition to its geometrical and material properties, each member is characterized by hydrodynamic coefficients, e.g., relating to drag, inertia, and marine growth, to allow wave forces to be automatically generated. Integrated decks and hulls of floating platforms, involving large bulkheads, are described by plate elements. The characteristics assumed for the plate elements depend on the principal state of stress to which they are subjected. Membrane stresses are taken when the element is subjected merely to axial load and shear. Plate stresses are adopted when bending and lateral pressure is to be taken into account. After developing a preliminary model for analysis, member stresses are checked for preliminary sizing under different environmental loads.

Verification of an element consists of comparing its characteristic resistance(s) to a design force or stress. It includes (i) a strength check where the characteristic resistance is related to the yield strength of the element; and (ii) a stability check for elements in compression where the characteristic resistance relates to the buckling limit of the element. An element (member or plate) is checked at typical sections (at least both ends and mid span) against resistance and buckling. This verification also includes the effect of water pressure for deep-water structures. Tubular joints are checked against punching under various load patterns. These checks may indicate the need for local reinforcement of the chord using over-thickness or internal ring-stiffeners. Elements should also be verified against fatigue, corrosion, temperature or durability wherever relevant.

2.18.2 Allowable Stress Method

This method is presently specified by American codes. The loads remain unfactored and a unique coefficient is applied to the characteristic resistance to obtain an allowable stress as shown in Table 2.5.

Table 2.5 Coefficient for resistance to stresses

Condition	Axial	Strong axis bending	Weak axis bending
Normal	0.60	0.66	0.75
Extreme	0.80	0.88	1.00

"Normal" and "extreme" respectively represent the most severe conditions under which (a) the plant is to operate without shutdown; and (b) the platform is to endure over its lifetime.

2.18.3 Limit State Method

This method is enforced by European and Norwegian authorities and has now been adopted by American Petroleum Institute (API) as it offers a more uniform reliability. Partial factors are applied to the loads and to the characteristic resistance of the element as given in Table 2.6. They reflect the amount of confidence placed in the design value of each parameter and the degree of risk accepted under a limit state as discussed below

- Ultimate limit state (ULS), which corresponds to an ultimate event considering the structural resistance with appropriate reserve.
- Fatigue limit state (FLS), which relates to the possibility of failure under cyclic loading.

Table 2.6 Load factors

Limit state	Load categories				
	P	*L*	*D*	*E*	*A*
ULS (normal)	1.3	1.3	1.0	0.7	0.0
ULS (extreme)	1.0	1.0	1.0	1.3	0.0
FLS	0.0	0.0	0.0	1.0	0.0
PLS (accidental)	1.0	1.0	1.0	1.0	1.0
PLS (post-damage)	1.0	1.0	1.0	1.0	0.0
SLS	1.0	1.0	1.0	1.0	0.0

Where, the following explanations are applicable
P represents permanent loads (structural weight, dry equipment, ballast, hydrostatic pressure)
L represents live loads (storage, personnel, liquid)
D represents deformations (out-of-level supports, subsidence)
E represents environmental loads (wave, current, wind, earthquake)
A represents accidental load (dropped object, ship impact, blast, fire). The material partial factors for steel are normally taken equal to 1.15 for ULS and 1.00 for PLS and SLS design. Guidance for classifying typical conditions into typical limit states is given in Table 2.7

Table 2.7 Conditions specified for various limit states

Conditions	Loadings				Design criterion
	P/L	*E*	*D*	*A*	
Construction	*P*				ULS, TSLS
Load-out	P	Reduced wind	Support displacement		ULS
Transport	*P*	Transport wind and wave			ULS
Tow-out (accidental)	*P*			Flooded compartment	PLS
Launch	*P*				ULS
Lifting	*P*				ULS
In-Place (normal)	$P + L$	Wind, wave and snow	Actual		ULS, SLS
In-Place (extreme)	$P + L$	Wind and 100 year wave	Actual		ULS, SLS
In-Place (exceptional)	$P + L$	Wind and 10,000 year wave	Actual		PLS
Earthquake	$P + L$	10^{-2} quake			ULS
Rare earthquake	$P + L$	10^{-4} quake			PLS
Explosion	$P + L$			Blast	PLS
Fire	$P + L$			Fire	PLS
Dropped object	$P + L$			Drill collar	PLS
Boat collision	$P + L$			Boat impact	PLS
Damaged structure	P + reduced L	Reduced wave and wind			PLS

- Progressive collapses limit state (PLS), which reflects the ability of the structure to resist collapse under accidental or abnormal conditions.
- Serviceability limit state (SLS), which corresponds to the criteria for normal use or durability (often specified by the plant operator).

The analysis of the offshore platform is an iterative process, which requires progressive adjustment of the member sizes with respect to the forces they transmit, until a safe and economical design is achieved. It is therefore of utmost importance to start the main analysis from a model which is close to the final optimized one. The simple rules given below provide an easy way of selecting realistic sizes for the main elements of offshore structures in moderate water depth (up to 80 m) where dynamic effects are negligible.

Jacket Pile Sizes

- Calculate the vertical resultant (dead weight, live loads, and buoyancy), the overall shear and the overturning moment (environmental forces) at the mudline.
- Assuming that the jacket behaves as a rigid body, derive the maximum axial and shear force at the top of the pile.
- Select a pile diameter in accordance with the expected leg diameter and the capacity of pile-driving equipment.
- Derive the penetration from the shaft friction and tip bearing diagrams.
- Assuming an equivalent soil sub grade modulus and full fixity at the base of the jacket, calculate the maximum moment in the pile and derive its wall thickness.

Deck Leg Sizes

- Adapt the diameter of the leg to that of the pile.
- Determine the effective length from the degree of fixity of the leg into the deck (depending upon the height of the cellar deck).
- Calculate the moment caused by wind loads on topsides and derive the appropriate thickness.

Jacket Bracings

- Select the diameter in order to obtain a span/diameter ratio between 30 and 40.
- Calculate the axial force in the brace from the overall shear and the local bending caused by the wave assuming partial or total end restraint.
- Derive the thickness such that the diameter/thickness ratio lies between 20 and 70 and eliminate any hydrostatic buckle tendency.

Deck Framing

- Select spacing between stiffeners (typically 500–800 mm).
- Derive the plate thickness from formulae accounting for local plastification under the wheel footprint of the design forklift truck.
- Determine by straight beam formulae the sizes of the main girders under "blanket" live loads and/or the respective weight of the heaviest equipment.

The static in-place analysis is the basic and generally the simplest of all analyses. The structure is modeled as it stands during its operational life and subjected to pseudo-static loads. This analysis is always carried at the very early stage of the project, often from a simplified model, to size the main elements of the structure. The main model should account for eccentricities and local reinforcements at the joints. For example, a typical model for North Sea jacket may feature over 800 nodes and 4000 members. The contribution of appurtenances like risers, J-tubes, caissons, conductors, boat-fenders, etc., to the overall stiffness of the structure is normally neglected. They are therefore analyzed separately and their reactions applied as loads at the interfaces with the main structure. Since their behavior is nonlinear, foundations are often analyzed separately from the structural model. They are represented by an equivalent load-dependent secant stiffness matrix; coefficients are determined by an iterative process where the forces and displacements at the common boundaries of structural and foundation models are equated. This matrix may need to be adjusted to the mean reaction corresponding to each loading condition. The static in-place analysis is performed under different conditions where the loads are approximated by their pseudo-static equivalent. The basic loads relevant to a given condition are multiplied by the appropriate load factors and combined to produce the most severe effect in each individual element of the structure. A dynamic analysis is normally mandatory for every offshore structure, but can be restricted to the main modes in the case of stiff structures.

2.19 Fabrication and Installation Loads

These loads are temporary and arise during fabrication and installation of the platform or its components. During fabrication, various structural components generate lifting forces, while in the installation phase forces are generated during platform load-out, transportation to the site, launching and upending, as well as during lifts related to installation. According to the Det Norske Veritas (DNV 1982) rules, the return period for computing design environmental conditions for installation and fabrication loads is three times as that of the duration of the corresponding phase. API-RP2A, on the other hand, leaves this design return period up to the owner, while the BS6235 rules recommend a minimum recurrence interval of 10 years for the design environmental loads associated with transportation of the structure to the offshore site.

2.20 Lifting Force

Lifting forces are functions of the weight of the structural component being lifted, the number and location of lifting eyes used for the lift, the angle between each sling and the vertical axis and the conditions under which the lift is performed, as shown in Fig. 2.14. All members and connections of a lifted component must be designed for the forces resulting from static equilibrium of the lifted weight and the sling tensions. Moreover, API-RP2A recommends that in order to compensate for any side movements, lifting eyes and the connections to the supporting structural members should be designed for the combined action of the static sling load and a horizontal force equal to 5% this load, applied perpendicular to the member at the center of the pinhole. All these design forces are applied as static loads if the lifts are performed in the fabrication yard. If, however, the lifting derrick or the structure to be lifted is on a floating vessel, then dynamic load factors should be applied to the static lifting forces. A factor of 2 is applied for members and connections and 1.35 for all other secondary members. For load-out at sheltered locations, the

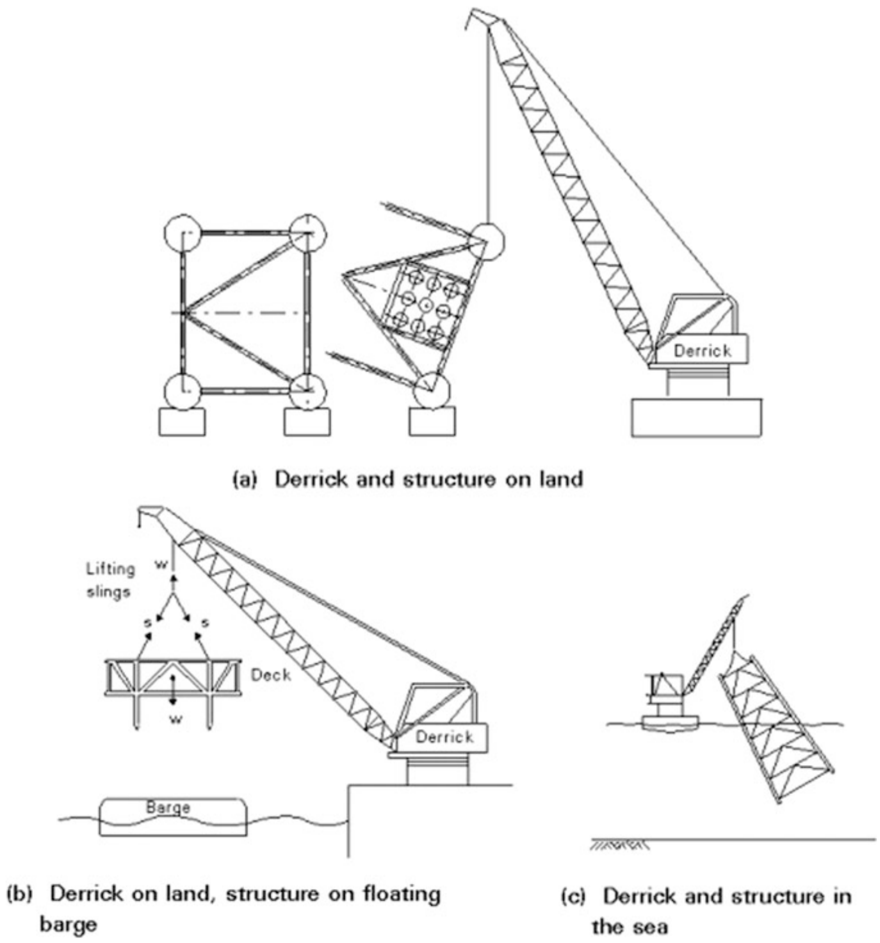

Fig. 2.14 Lifts under different conditions

corresponding minimum load factors for the two groups of structural components are 1.5 and 1.15, respectively.

2.21 Load-Out Force

These are forces generated when the jacket is loaded from the fabrication yard onto the barge. If the load-out is carried out by direct lift, then, unless the lifting arrangement is different from that to be used for installation, lifting forces need not be computed. This is because lifting in the open sea creates a more severe loading condition, which requires higher dynamic load factors. If load-out is done by skidding the structure onto the barge, a number of static loading conditions must be considered, with the jacket supported on its side. Such loading conditions arise from the different positions of the jacket during the load-out phases as shown in Fig. 2.15. Since movement of the jacket is slow, all loading conditions can be taken as static.

Typical values of friction coefficients for the calculation of skidding forces are: (i) steel on steel without lubrication (0.25); (ii) steel on steel with lubrication (0.15); (iii) steel on Teflon (0.10); and (iv) Teflon on Teflon (0.08). A typical ballast and displacement values are indicated in the figure.

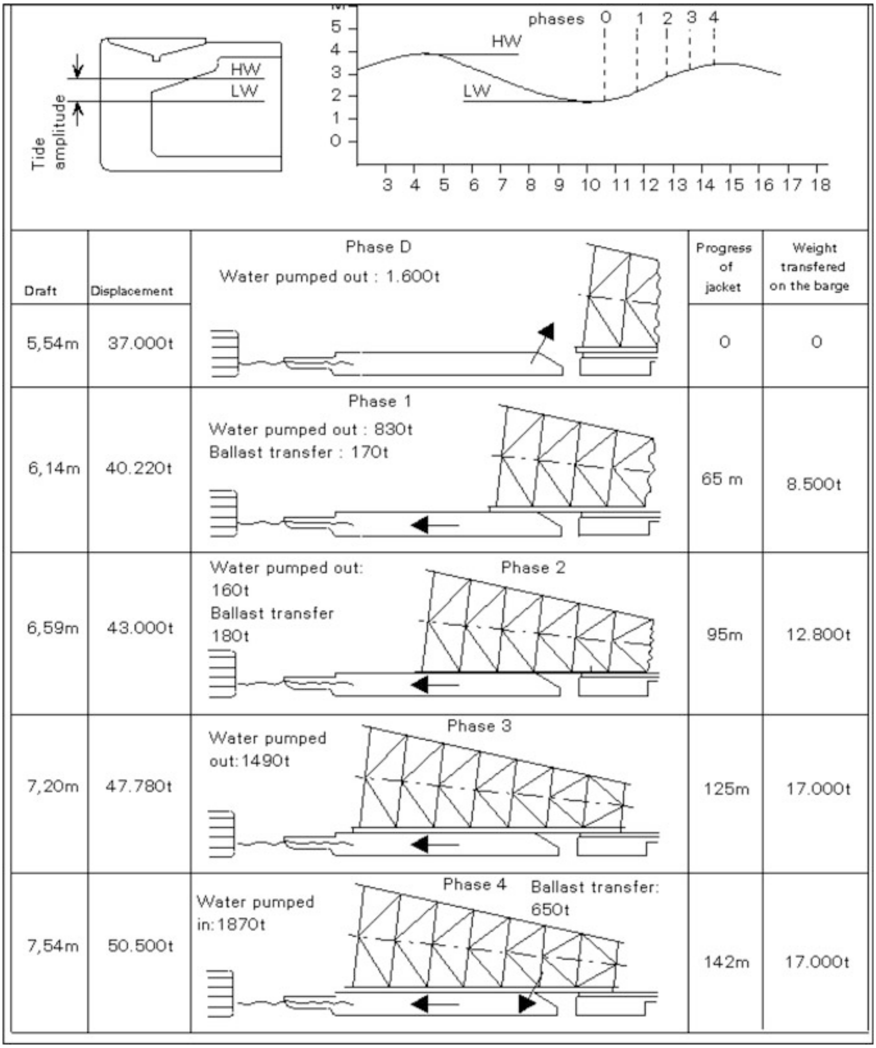

Fig. 2.15 Different phases of jacket load-out by skidding

2.22 Transportation Forces

These forces are generated when platform components (jacket, deck) are transported offshore on barges or self-floating. They depend upon the weight, geometry and support conditions of the structure (by barge or by buoyancy) and also on the environmental conditions (waves, winds, and currents) that are encountered during transportation. The types of motion that a floating structure may experience are shown schematically in Fig. 2.16.

In order to minimize the associated risks and secure safe transport from the fabrication yard to the platform site, it is important to plan the operation carefully by considering the following (API-RP2A):

- Previous experience along the tow route
- Exposure time and reliability of predicted "weather windows"
- Accessibility of safe havens

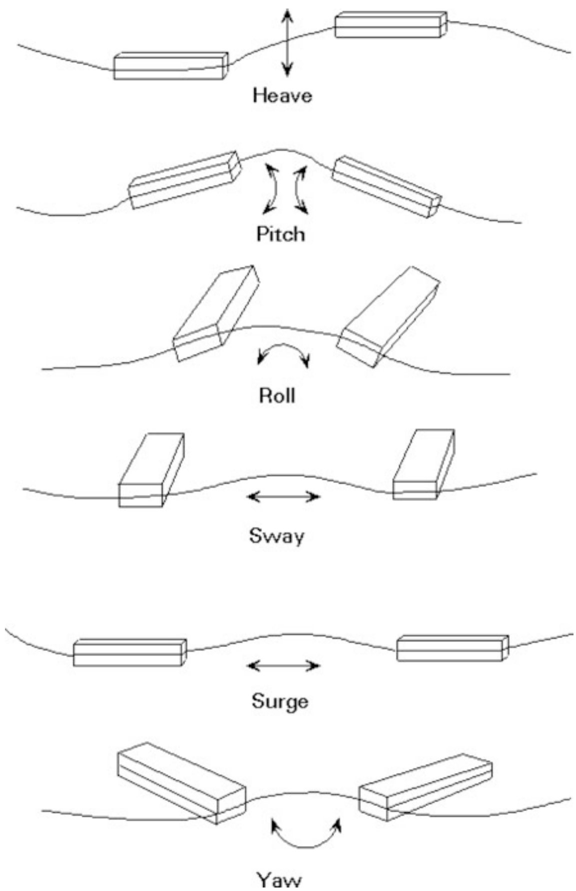

Fig. 2.16 Motion of floating objects during installation

- Seasonal weather system
- Appropriate return period for determining design wind, wave and current conditions, taking into account the characteristics of the tow such as size, structure, sensitivity and cost.

The motion of the tow, i.e., the structure and supporting barge, generates transportation forces. They are determined from the design winds, waves and currents. If the structure is self-floating, the loads are calculated directly. According to API-RP2A, towing analyses must be based on the results of model basin tests or appropriate analytical methods and must consider wind and wave directions parallel, perpendicular and at 45° to the tow axis. Inertial loads shall be computed from a rigid body analysis of the tow by combining roll and pitch with heave motions, when the size of the tow, magnitude of the sea state and experience make such assumptions reasonable. For open sea conditions, typical values are 20° (for single amplitude roll motion) and 10° for single amplitude pitch motion. The period of roll or pitch is taken as 10 s, while heave acceleration is taken as 0.2 g. When transporting a large jacket by barge, stability against capsizing is a primary design consideration because of the high center of gravity of the jacket. Moreover, the relative stiffness of jacket and barge may need to be taken into account together with the wave slamming forces that could result during a heavy roll motion of the tow, as shown in Fig. 2.17. Structural analyses are carried out for designing the tie-down braces and the jacket members affected by the induced loads.

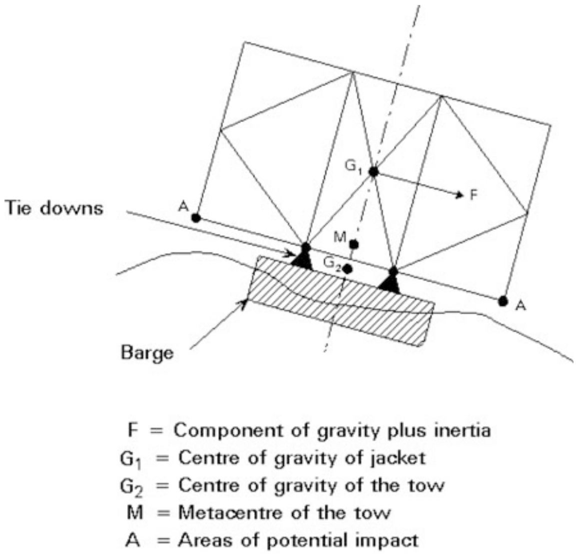

Fig. 2.17 View of launch barge and jacket undergoing motion

2.23 Launching and Upending Force

These forces are generated during the launch of a jacket from the barge into the sea and during the subsequent upending into its proper vertical position to rest on the seabed. A schematic view of the five stages the operation can be seen in Fig. 2.18.

Five stages in a launch-upending operation are (i) jacket slides along the skid beams; (ii) jacket rotates on the rocker arms; (iii) jacket rotates and slides simultaneously; (iv) detaches completely and comes to its floating equilibrium position; and (v) jacket is upended by a combination of controlled flooding and simultaneous lifting by a derrick barge. Both the static and dynamic loads for each stage of the above under the action of wind, waves and current need to be included in the analysis. To start the launch, the barge must be ballasted to an appropriate draft and trim angle and subsequently the jacket must be pulled towards the stern by a winch. Sliding of the jacket starts as soon as the downward force (gravity component and winch pull) exceeds the friction force. As the jacket slides, its weight is supported on the two legs that are part of the launch trusses. The support length keeps decreasing and reaches a minimum, equal to the length of the rocker beams, when rotation starts. It is generally at this instant that the most severe launching forces develop as reactions to the weight of the jacket. During the last two stages, variable hydrostatic forces arise, which have to be considered at all members affected. Buoyancy calculations are required for every stage of the operation to ensure fully controlled, stable motion. Computer programs are available to perform the stress analyses required for launching and upending and also to portray the whole operation graphically.

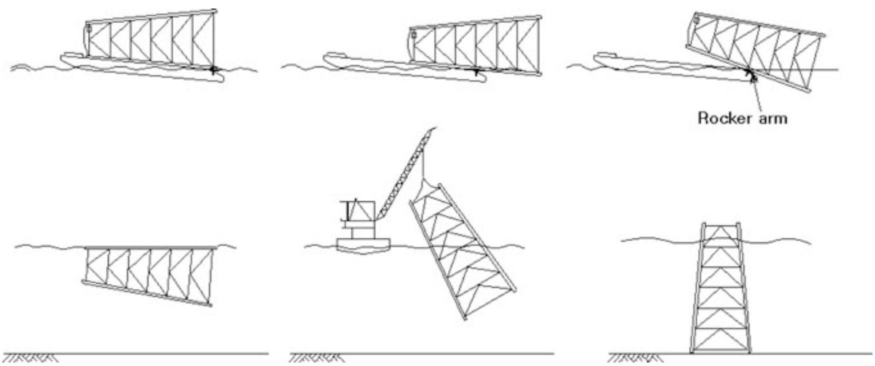

Fig. 2.18 Launching and upending

2.24 Accidental Load

According to the DNV rules, accidental loads are ill-defined with respect to intensity and frequency, which may occur as a result of an accident or exceptional circumstances. Examples of accidental loads are loads due to collision with vessels, fire or explosion, dropped objects, and unintended flooding of buoyancy tanks. Special measures are normally taken to reduce the risk from accidental loads. For example, protection of wellheads or other critical equipment from a dropped object can be provided by specially designed, impact resistant covers. An accidental load can be disregarded if its annual probability of occurrence is less than 10^{-4}. This number is the estimate of order of magnitude and is extremely difficult to compute.

Exercise
PART A

1. The design of offshore structures are dominated by ___________.
2. Earthquakes are normally regarded as ___________ loads in offshore engineering.
3. The mean recurrence interval of a design event is called ___________.
4. The wind pressure coefficient is calculated from ___________.
5. The coefficient of wind pressure depends upon __________.
6. The gust component of wind is generated by __________.
7. Wind force in the direction parallel and normal to the wind direction are called __________ and __________ respectively.
8. The one minute average wind speed according to U.S. weather bureau is called ___________.
9. The one-seventh power law is used to calculate __________ of wind speed.
10. Wave forces causes ___________ and ___________, while earthquake forces causes __________ on the members.
11. In slender and flexible members, the de-amplification takes place due to __________.
12. ___________ is used to define the cross-spectrum in the analysis.
13. Aerodynamic admittance function connects _________ and __________.
14. For the analysis of high-frequency wind data, ________ spectrum is used.
15. Harris spectrum is not recommended for the frequencies __________.
16. _____________ gives a better fit to empirical observations of atmospheric turbulence.
17. Linear theory is applied when H/gT^2 is ___________.
18. Airy's theory is valid only up to __________.
19. PM spectrum is recommended for _________ conditions.
20. For North Sea, ___________ spectrum is recommended.
21. The sea state in short term is assumed as ____________.
22. ___________ describes the energy distribution of different frequencies of a sea state.

23. PM spectrum is used for ___________ condition, which is neither _______, nor ___________.
24. __________ spectrum has a greater frequency bandwidth compared to PM spectrum.
25. Bredneidger spectrum is usually used to describe _______ waves, generated by _________.
26. ___________ spectrum is a modification of Bredneidger spectrum, and is true only for _________.
27. JONSWAP spectrum is recommended for use in _________ analysis.
28. Peakedness parameter follows ___________ distribution.
29. ___________ is caused by the pressure effects due to undisturbed incident waves.
30. ___________ is caused by the pressure effects due to the presence of the structure in the fluid domain.
31. __________ and ___________ is cause by the pressure effects due to the motion of the structural components in _________.
32. __________ is caused by the pressure effects due to the relative velocity between the water particle and the structural component.
33. For slender structures, ___________ and ___________ are idealized as a single inertia term.
34. Reaction forces developed due to acceleration and velocity results in ____________ and __________ respectively.
35. The relative velocity of the structure in the fluid produces __________ and ____________.
36. In large diameter members, ________ becomes less significant.
37. Force is calculated by _________ method using the incident wave pressure that is acting on the ___________ of the structure.
38. The opposing current will _________ the wave height and ______ the wave length.
39. The superposing current will _________ the wave height and ______ the wave length.
40. The opposing current will __________ the force and supposing current will _______ the force on the member.
41. Current affects the _______ force component only.
42. Current force should be added vectorially to ____________ before calculating ___________.
43. Current causes the structure to generate _______, which inturn creates _________.
44. Compliant structures that are position-restrained by tethers will be subjected to _____________ under the presence of earthquake forces.
45. Earthquake will cause motion for a typical duration of __________.
46. Earthquake can result in _________ due to ____________ and ____________.
47. Dynamic tether tension variation caused by the earthquake forces are in the order of about __________ more than that of the normal values.

48. __________ is important to quantify the ice loads n the offshore structure.
49. Total ice force can result in _____________ and can cause _____________ in flexible structures.
50. Extreme static ice loads depends upon ____________ of the structure.
51. Ice loads in _______________ are lesser than that of the cylindrical structure.
52. Well-defined cone shape can change the ice-failure mode from ___________ to ____________.
53. ____________ is the most practical way to estimate the ice loads.
54. In the frequency domain approach, excitation caused by ice loads is modeled as ___________, and the response is characterized by the ____________.
55. Marine growth increases ____________ and ____________ of the structure.
56. Marine growth results in ___________ gravity loads.
57. Marine growth __________ drag coefficient due to ____________.
58. Added mass depends upon ________________ of the platform.
59. Mass is contributed by ___________ and ______________ of the structure.
60. In slender structures, _____________ should be considered in the analysis.
61. For steel offshore structures, structural damping varies from _____________ of that of the critical damping.
62. For concrete offshore structures, structural damping varies from _____________ of that of the critical damping.
63. Hydrodynamic damping originated from ____________ and ____________.
64. Radiation damping is determined based on ___________ and it depends upon __________ and ___________.
65. Drag damping is lower for _____________.
66. Total damping ratio is about ___________ for the first three modes of bottom-supported structures.
67. Dead load excludes ____________, ____________, ____________ and _____________.
68. Dynamic amplification factor is applied to _____________.
69. _______________ is lesser in bottom-supported structures.
70. In bottom-supported structures, the design criteria is to control ____________.
71. In compliant structures, the design criteria is to control ___________.
72. Orientation of the platform is altered to reduce ____________ and ___________.
73. ____________ should be considered when the elements are subjected to axial load and shear.
74. When the elements are subjected to bending and lateral pressure, __________ should be considered in the analysis.
75. Tubular joints in steel offshore platforms should be checked for ___________ under various load patterns.
76. Fatigue limit state relates the possibility of failure under _____________.
77. _____________ corresponds to the criteria for normal use or durability.
78. ___________ is the basic simplest analysis procedure, where the loads are approximated by ____________.

79. According to BS6235, the mean recurrence interval associated with the transportation of the structure is ____________.
80. According to DNV, the return period for computing design environmental conditions for installation and fabrication is _________.
81. Lifting forces on the structures are functions of _________, ________, _______ and ___________.
82. The members and connections of the lifted component must be designed for the forces resulting from ______ and ________.
83. If the structure is lifted in fabrication yard, the design forces are applied as _________.
84. The minimum load factors that must be considered for the members and connections for load-out at sheltered locations are _________ and _________ respectively.
85. Lifting in open sea creates _________ which requires ___________.
86. Load-out is carried out by _______ and __________.
87. Transportation forces depends upon _________, __________ and __________ of the structure.
88. The offshore structures are transported by ___________ and __________.
89. During floating transportation, the structure will undergo _________.
90. According to API-RP2A, the period of roll or pitch in towing analysis is ________.
91. ____________ is the primary consideration while transporting a large jacket by barge, because of the ___________.
92. _____________ and ____________ should be considered while transporting the jacket platforms.
93. __________ is considered important in every stage of launch operation for fully controlled stable motion.
94. Accidental loads occurs sue to _________, __________, ____________ and ____________.
95. Fire resistance to structures are provided in the form of ______________.
96. An accidental load can be disregarded if its annual probability of occurrence is ___________.

PART B

1. List type of loads that act on offshore structures.
2. List various environmental loads that act on offshore structure.
3. How wind forces are estimated on offshore structures?
4. What are the two components of wind?
5. In offshore structures, static wind analysis is sufficient. State true or false with reason.
6. Explain the spatial dependence of the components of wind.
7. Mention the law, used to calculate the wind speed. Explain why it is widely used?

8. How the mean and gust components of wind speed were calculated?
9. What is fastest mile velocity?
10. The effect of waves and earthquake on the structure is different. Why?
11. What are the parameters to be considered while considering wind as a dynamic process?
12. Name the function which is used to handle the spatial variations of the wind velocity. State the importance of the function.
13. How the standard wind data is measured?
14. Name few wind spectra used in the design of offshore structures.
15. State the importance of gust component of wind speed in offshore structures.
16. The application of Davenport spectrum and Harris spectrum to offshore structures is questionable. Why?
17. Plot the variation of spectral density for wind spectra and state the inferences.
18. How the wind-generated sea surface is represented?
19. List the different wave theories.
20. Why Airy's wave theory is commonly used?
21. How the additional forces due to variable submergence are accounted for, in Airy's theory?
22. How the wave data is collected?
23. How the sea state is assumed in short-term- and long-term processes?
24. Under what conditions, PM spectrum is used?
25. Where will you recommend the usage of JONSWAP spectrum?
26. Compare the different wave spectra and state the inferences.
27. How the compliancy of the structure is considered while calculating the wave forces?
28. Mention the parameters based on which the drag and inertia components are calculated?
29. Mention the recommended values of drag and inertia coefficients according to API RP 2A.
30. Why Morison equation is not recommended for large diameter structures?
31. Why the spacing between the columns in offshore structures is considered to be very important?
32. Find the phase angle for the typical topside of 100 × 100 m, resting on four columns. The wave period is 12 s. State whether cancelation of forces will occur or not.
33. Wave force is calculated by assuming that the structure does not distort the wave field in its vicinity. Why?
34. What are the effects of current in the wave forces?
35. How the presence of the current is accounted in the design alternatively?
36. Show the variation of the total force in the presence and absence of current and state the inferences.
37. How earthquake affects the fixed and compliant structures?
38. Why earthquakes are considered to be random in nature?

39. Explain how earthquake forces are handled in the analysis of compliant structures?
40. Spectral density peak of earthquake forces increases with the decrease in the damping ratio. Validate the statement.
41. Mention the different forms of ice.
42. What are the different types of failure of offshore structures under ice loads?
43. Mention the classification of ice loads.
44. Why ice loads in conical structure are lesser than that of the cylindrical structure?
45. Mention the factors used for the design ice loads.
46. What are the advantages and disadvantages of the experimental analysis of structures subjected to ice loads?
47. What are the effects of the marine growth on the offshore structures?
48. How marine growth is accounted for in the design of the structure?
49. What is the significance of added mass in the analysis of the structure?
50. How stability is ensured during free-floating conditions? Why is it important?
51. Mention the different types of damping.
52. How to calculate the damping ratio for offshore structures?
53. Mention the dead loads acting on an offshore platform.
54. How live loads on offshore structures are designated?
55. Explain why the design methodology of the offshore platform differs based on the different types?
56. State the design criteria in bottom-supported and compliant structures.
57. How orientation of members plays an important role in the design?
58. How to check the safety of the steel structure?
59. List the different limit states considered in the design of offshore structures.
60. What are the steps involved in the calculation of the jacket pile sizes?
61. How to arrive at the optimum size of leg member in an offshore platform?
62. How jacket bracings are designed in offshore platforms?
63. List the fabrication and installation loads developed in the offshore structures.
64. How the members of the lifted components should be designed?
65. Mention the recommendations from API-RP2A for the design of the lifted structure.
66. How the design forces are applied, when the structure is lifted from a floating vessel?
67. What do you understand by load-out force?
68. How load-out analysis is performed under direct lift and skidding conditions?
69. Mention the recommendations from API for secure transport of the offshore structures.
70. What is the consequence of heave roll motion of the tow during transportation?
71. What are the steps involved in the installation of jacket platforms?
72. Hoe launching and upending forces are generated in the offshore structure?
73. What are the stages involved in the launch-upending operation?

74. What are the loads to be considered in the launch-upending operation?
75. When will the maximum launching force acts on a structure?

Key to Exercise
PART A

1. Environmental loads.
2. Environmental loads.
3. Return period.
4. Wind tunnel experiment.
5. Reynolds number.
6. Turbulence of the flow field.
7. Drag force and lift force.
8. Sustained wind speed.
9. Mean component.
10. Inertia and drag, inertia.
11. Compliancy.
12. Aerodynamic admittance function.
13. Force and response spectra.
14. Davenport.
15. Less than 0.1 Hz.
16. Kaimal spectrum.
17. Less than 0.01.
18. Mean sea level.
19. Opens sea.
20. JONSWAP.
21. Zero-mean ergodic process.
22. Wave spectra.
23. Fully developed sea, fetch limited, duration limited.
24. Bredsneidger.
25. Tropical storm, hurricanes.
26. ISSC, narrow-banded spectrum.
27. Reliability.
28. Normal probability.
29. Froude-Krylov forces.
30. Diffraction force.
31. Hydrodynamic added mass and potential damping force, ideal fluid.
32. Viscous drag force.
33. Froude-Krylov forces and Diffraction force.
34. Inertia force and potential damping force.
35. Excitation and damping forces.
36. Viscous force.
37. Pressure area method, submerged surface.
38. Increase, decrease.

39. Decrease, increase.
40. Increase, decrease.
41. Drag.
42. Horizontal water particle velocity, drag force.
43. Waves, diffraction forces.
44. Dynamic tether tension variations
45. 15–30 s.
46. Inertia forces, acceleration and damping.
47. 65%
48. Number of interactions per unit time.
49. Periodic loading, dynamic amplification.
50. Geometric shape.
51. Conical structure.
52. Crushing, bending.
53. Data mining.
54. Sinusoidal pseudo-excitation, transfer function.
55. Diameter, roughness.
56. Higher.
57. Increases, roughness.
58. Submerged volume.
59. Structural mass, hydrodynamic added mass.
60. Mass of the displaced volume.
61. 0.2–0.5%.
62. 0.5–1.5%.
63. Radiation and viscous damping.
64. Potential theory, frequency and submergence effects.
65. Large diameter column members.
66. 2%.
67. Weight of drilling equipment, production equipment, drilling supplies and treatment supplies.
68. Live loads.
69. Vertical deformation.
70. Stresses.
71. Displacement.
72. Projected area, response.
73. Membrane stresses.
74. Plate stresses.
75. Punching.
76. Cyclic loads.
77. Serviceability limit state.
78. Static in-place analysis, pseudo-static equivalent.
79. 10 years.
80. Three times as that of the duration of the corresponding phase.

81. Weight of the structure, number and location of lifting eyes, angle of lifting and conditions under which the lift is performed.
82. Static equilibrium of the lifted weight and sling tensions.
83. Static loads.
84. 1.5 and 1.15.
85. Severe loading condition, higher load factors.
86. Direct lift and skidding.
87. Weight, geometry and support conditions of the structure.
88. Derrick barges and self-floating.
89. Surge, sway, heave, roll, pitch and yaw.
90. 10 s.
91. Stability against capsizing, high center of gravity of the jacket.
92. Relative stiffness of jacket and barge, wave slamming forces.
93. Buoyancy.
94. Collision with vessels, fire or explosion, dropped objects and unintended flooding of buoyancy tanks.
95. Passive fire protection.
96. Less than 10^{-4}.

PART B

1. Permanent loads or dead loads, Operating loads or live loads, Other environmental loads including earthquake loads, Construction and installation loads and Accidental loads.
2. Wind, waves, current, tides, earthquakes, temperature, ice, seabed movement and marine growth.
3. Most widely used engineering approaches to estimate wind forces on offshore structures are based on few observations as listed below
   - When stream of air flows with constant velocity (v), it will generate force on the flat plate of area (A).
   - The plate will be placed orthogonal to the flow direction.
   - This force will be proportional to (Av^2).
   - The proportionality constant is independent of the area, which is verified by experimental studies.
4. Natural wind has two components: (i) mean wind component (which is static component); and (ii) fluctuating, gust component (which is a dynamic component).
5. For offshore locations, mean wind speed is much greater than the gust component, which means that in most of the design cases, a static analysis will suffice.
6. The spatial dependence of the mean component is only through the vertical coordinate, while $v(t)$ is homogeneous in both space and time.
7. Wind spectrum above water surface is given by one-seventh power law, which is

$$v_z = V_{10}\left[\frac{z}{10}\right]^{\frac{1}{7}} \tag{2.5}$$

where v_z is the wind speed at elevation of z m above MSL, V_{10} is the wind speed at 10 m above MSL, and 10 m is called the reference height. Power law is purely empirical and most widely used. It is tested with the actual field measurements and found to be in good agreement.

8. One-seventh power law is used to calculate the mean component of wind speed. The gust component can be obtained by multiplying a gust factor with the sustained wind speed. Average gust factor (F_g) is in the range of 1.35–1.45; variation of the gust factor along the height is negligible.
9. The product of sustained wind speed and the gust factor will give the *fastest mile velocity*.
10. Wave forces alone acting on the member will cause inertia and drag forces, while earthquake forces cause only inertia forces on the members. Hence, vibration of the structure induced by wind and waves are different from that caused by earthquakes.
11. While considering wind as a dynamic process, the following parameters are important:

    - Length of the record: The record can be continuous, intermittent or select record whose values are above the threshold value. For the record to be continuous, average values of the wind velocity is lesser than that of the intermittent because of the longer length of the record when compared with the former.
    - Wind spectrum: It is used as input for the structural analysis, which defines the fluctuating wind component.
    - Gust component: It is approximated by the *aerodynamic admittance function*.

12. There are two reasons for using the aerodynamic admittance function: (i) to bypass the rigorous random analysis; and (ii) possibility of an accurate measurement of this function through wind tunnel experiments. In this manner, the spatial variations of wind velocity are handled intelligently in the design.
13. The standard wind data represents 10 min average speed measured on mean sea level (DNV report). Wind instruments are mounted on light houses, ships, at fixed positions at sea approximately 4 m above sea level.
14. Davenport, Harris, Kaimal and API (2000) spectrum.
15. Steady wind forces are calculated from time averaged wind speed. However, fluctuating gust component may lead to resonating oscillations in offshore structures.
16. It is important to note that none of these spectrum used in the analysis of wind speed is recorded offshore; they are based on onshore records. Hence these applications to offshore locations are questionable. They have serious problem when used for low-frequency flexible structures.

17. Wind spectra plot

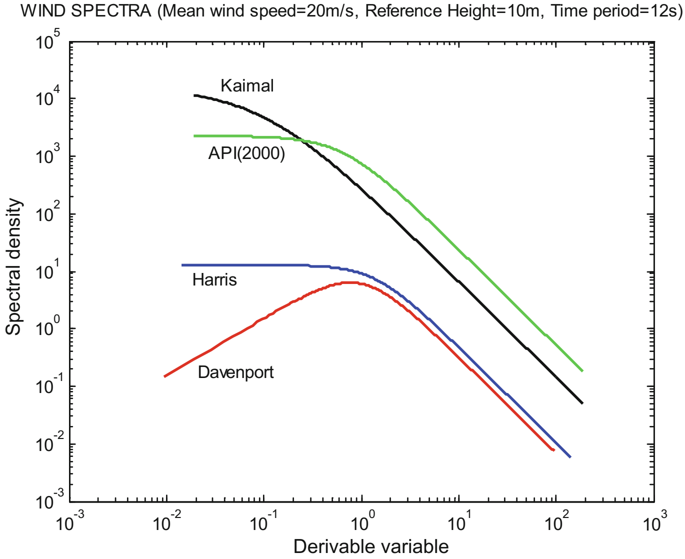

18. Wind-generated sea surface waves can be represented by a combination of regular waves. Regular waves of different magnitude and wave lengths from different directions are combined to represent the sea surface elevation.
19. Linear or first-order or Airy theory
    Stokes fifth-order theory
    Solitary wave theory
    Cnoidal theory
    Dean's stream function theory
    Numerical theory by Chappelear
20. Among all the theories, Airy's wave theory is commonly used because it assumes linearity between the kinematic quantities and the wave height, which makes the wave theory simple.
21. Airy's theory is valid up to mean sea level only. However, due to the variable submergence effect, the submerged length of the members will be continuously changing. This will attract additional forces due to their variable submergence at any given time. To compute the water particle kinematics up to the actual level of submergence, stretching modifications suggested by various researchers are used.

- Wheeler suggested the following modification in the horizontal water particle velocity and acceleration to include the actual level of submergence of the member

$$\dot{u}(x,t) = \frac{\omega H}{2} \frac{\cosh\left(ky\left[\frac{\mathrm{d}}{\mathrm{d}+\eta}\right]\right)}{\sinh(kd)} \cos(kx - \omega t)$$
$$\ddot{u}(x,t) = \frac{\omega^2 H}{2} \frac{\cosh\left(ky\left[\frac{\mathrm{d}}{\mathrm{d}+\eta}\right]\right)}{\sinh(kd)} \sin(kx - \omega t)$$

- Chakrabarti suggested the modification as given below

$$\dot{u}(x,t) = \frac{\omega H}{2} \frac{\cosh(ky)}{\sinh(k(\mathrm{d}+\eta))} \cos(kx - \omega t)$$
$$\ddot{u}(x,t) = \frac{\omega^2 H}{2} \frac{\cosh(ky)}{\sinh(k(\mathrm{d}+\eta))} \sin(kx - \omega t)$$

22. Wave data are collected are approximately collected for 20 min every 3 h and assumed to represent the stationary sea state between the measurements. The sea state is defined by significant wave height, significant wave period, peak period, and wave direction. Data collection is done by visual investigation and instrumental observations by buoys, radars, lasers, and satellites.
23. The sea state, in a short term, which is typically 3 h, is assumed as zero mean, ergodic Gaussian process. In a long term, variation of sea state is slower than the short-term fluctuations. It is often approximated by a series of stationary, nonzero-mean Gaussian process, which is specified by the significant wave height (H_s) and peak wave period (T_p).
24. PM spectrum is a one parameter spectrum and it used for fully developed sea condition as generated by relatively moderate winds over large fetches.
25. JONSWAP spectrum is a modified form of PM spectrum and it is recommended for use in the reliability analysis. This spectrum is applicable only for limited fetch and it is used to describe the winter storm waves of the North Sea.
26. Wave spectra plot

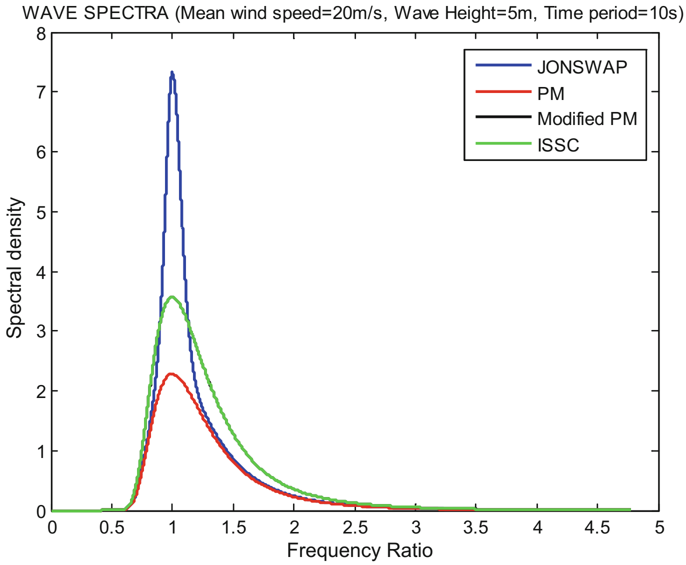

27. If the structure is compliant, the added mass forces associated with the relative acceleration between the fluid particles and the structures are included. Drag force will be computed by replacing the water particle velocity with the relative velocity term.
28. flow conditions, Keulegan–Carpenter number and Reynolds number.
29. The recommended value of drag coefficient is 0.6–1.2, while that of the inertia coefficient is 1.2–2.0, as seen in the literature (APR RP 2A).
30. As in the case of bottom-supported structures (gravity platforms), when the diameter of the member is very large, incident waves are disturbed by the presence of the structure. In such cases, viscous force becomes less significant due to the smaller values of the ratio of wave height to member diameter ($H/D \ll 1$). In such cases, the above equations cannot be applied; it is recommended that the analyzer should use numerical methods to determine the forces on the members.
31. Offshore structures have large plane area. Larger topside is required for accommodating the equipment layout as discussed in the previous chapter. As the deck will be supported on a few column members in order to reduce the interference of the waves by the presence of column members, their spacing plays an important role. For a large spacing of *c*/*c* distance of column members, there can be cancelation of forces.
32. Phase angle (θ) is given by the following relationship:

$$\theta = \frac{2\pi\Delta x}{\lambda}$$

Phase angle = 0.89π. Hence there is no cancelation effect.

33. For a small structure, Morison equation is valid because the flow structure is complex. However, for large structures (relative to the wavelength) the flow remains essentially attached to the surface. It is therefore easier to compute this pressure field. If the computation of the scattered wave potential is waived and its effect is incorporated by a force coefficient, then this force is called the *Froude-Krylov* force. Thus, the calculation of the force is performed assuming that the structure does not distort the wave field in its vicinity.
34. Current decreases slowly with the increase in depth, but even a small magnitude of current velocity can cause significant drag force. The opposing current will increase the force on the member and the superposed current will decrease the total force. The effect of current on the variation of total force with respect to phase angle is shown in the figure.
35. The presence of current is alternatively accounted by increasing the wave height to 10–15% and neglect the presence of current per second.
36. Influence of phase angle.

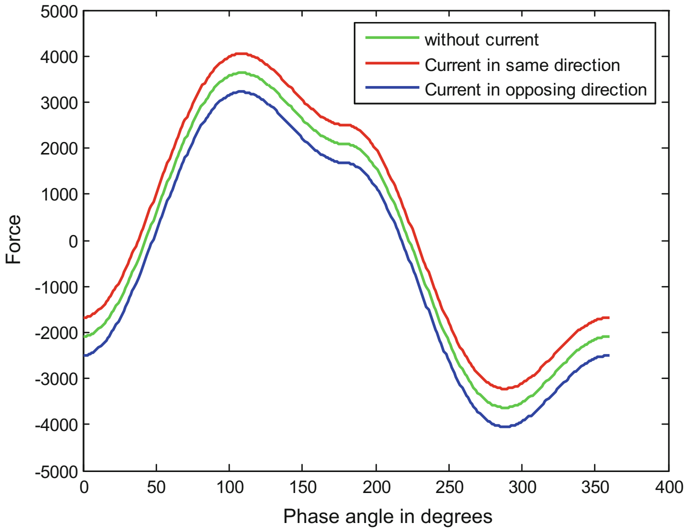

37. Offshore platforms which do not have stiff connection with the seabed are indirectly influenced by earthquakes; those which are bottom-supported are affected by earthquakes directly. Compliant structures that are position-restrained by tethers will be subjected to dynamic tether tension variations under the presence of earthquake forces. This will give rise to the

dynamic tether tension variations, which in turn shall affect the response of the platform under lateral loads.

38. Earthquake acceleration exhibits random characteristics due to (i) the nature of the mechanism causing earthquakes; (ii) wave propagation; (iii) reflection; and (iv) deflection.
39. In case of the analysis of compliant structures like TLPs, earthquake forces are handled in an indirect manner. Water waves generated due to the ground motion are neglected. Stiffness of TLP tether is modeled as axial tension members; slackening of tethers is neglected. The dynamic tether tension variation, caused by the horizontal motion of the earthquakes, is used to update the stiffness matrix of the TLP using the following equation (Chandrasekaran and Gaurav 2008):

$$\Delta T = \frac{AE}{\ell}\left[x(t) - x_{\mathrm{g}}(t)\right]$$

40. The spectrum plot shows the variation.

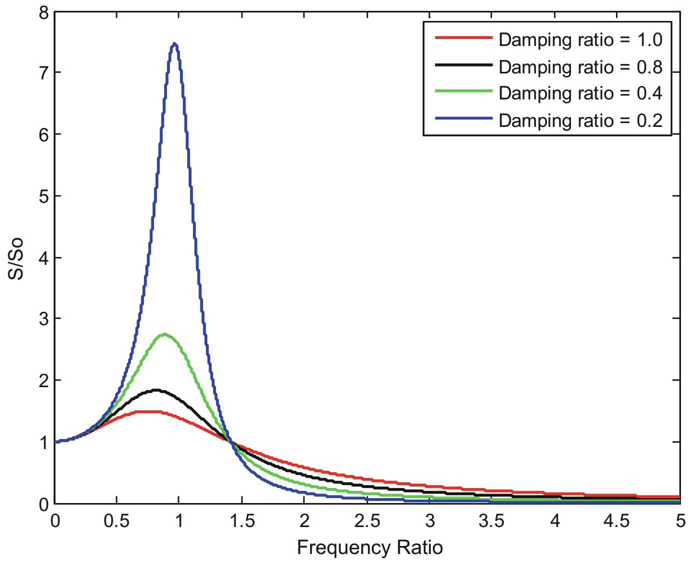

41. Level ice, broken ice, ice ridges, and icebergs.
42. Creep, cracking, buckling, spalling, and crushing.
43. (i) Total or global loads and (ii) local loads or pressure. Global loads affect the overall motion and stability of the platform, while local loads affect the members at connections.

44. Studies show that ice loads in a conical structure are lesser than that of the cylindrical structure. This is because a well-designed cone shape can change the ice-failure mode from crushing to bending.
45. The design ice loads use varying factors for level ice, first-year ridge ice and multi-year ridge ice; the factored values are 2, 5, and 7, respectively.
46. Experimental studies use scaling laws to determine the ice loads and ice–structure interaction. This method claims many advantages due to the capability of testing many types of structural shapes in large testing facilities. However, such tests are expensive apart from a strong disagreement of the model ice not being accurately scaled as of the sea ice. As the ice failure is dependent on the geometric shape significantly, ice-failure behavior cannot be accurately studied. This may result in over-prediction of ice loads.
47. Marine growth or bio-fouling is the ubiquitous attachments of soft and hard bio-particles on the surface of a submerged structure. It ranges from seaweeds to hard-shelled barnacles. Its growth on the surface of the structure increases its diameter and affects its roughness. Its main effect is to increase the wave forces on the members by increasing not only exposed areas and volumes, but also the drag coefficient due to higher surface roughness. In addition, it increases the unit mass of the member, resulting in higher gravity loads and in lower member frequencies.
48. It is accounted for in the design through appropriate increases in the diameters and masses of the submerged members.
49. Added mass depends on the submerged volume of the platform, which also varies with respect to period of vibration. This is due to the variation in buoyancy, which in turn changes the tether tension variation that affects the natural frequency of motion.
50. It is also important to establish the fact that a desired proportion between center of buoyancy and center of mass is maintained to ensure stability under free-floating conditions. This is important to enable smooth construction process in case of floating.
51. 1. Structural damping
    2. Hydrodynamic damping: Radiation and viscous damping.
52. Damping ratio for offshore structures (wet structures), including the effects of added mass, can be expressed as a ratio of that of the dry structures, as given below

$$\xi_{\mathrm{wet}} = \xi_{\mathrm{wet}} \frac{(m^*_{\mathrm{dry}})(\omega^*_{\mathrm{dry}})}{(m^*_{\mathrm{wet}})(\omega^*_{\mathrm{wet}})}$$

    where m^*, ω^* are generalized mass and frequency, respectively.
53. Dead load is the weight of the overall platform in air, which includes piling, superstructure, jacket, stiffeners, piping, conductors, corrosion anodes, deck, railing, grout and other appurtenances.

54. Live loads are generally designated as factor times of the applied static load. These factors are assigned by the designer depending on the type of platform.
55. Design methodology of offshore platforms differs with different types of offshore structures. For example, vertical deformation will be lesser in case of bottom-supported structures like jacket platform, GBS, etc. Such platforms are highly rigid and tend to attract more forces. Hence the design criteria should be to limit the stresses in the members. Displacement of the members under the applied loads will be insignificant. On the contrary, compliant structures are more flexible, as they all displaced more under wave action. They also create more disturbances in the waves. Hence the design criteria will be to control displacement instead of limiting the stresses in the members.
56. In bottom-supported structures, design criteria should be to limit the stresses in the member. In compliant platforms, the design criteria will be to control displacement.
57. Preferred orientation is that members are oriented to have less projected area to the encountered wave direction. This induces lesser response on the members. Predominant wave direction for the chosen site is made available to the designer based on which the platform orientation is decided.
58. Following are the list of data required for the design of offshore structures:

    - Land topographical survey of sufficient area covering the chosen site for platform installation.
    - Hydrographical survey of the proposed location (hydrographic charts are used for this purpose).
    - Information regarding silting at the site.
    - Wind rose diagram showing information on wind velocities, duration, predominant direction round the year.
    - Cyclonic tracking data showing details of the past cyclonic storm such that wind velocities, direction, peak velocity period, etc., are indicated.
    - Oceanographic data including general tide data, tide table, wave data, local current, seabed characteristics, temperature, rainfall, and humidity.
    - Seismicity level and values of acceleration.
    - Structural data of existing similar structures, preferably in the close vicinity.
    - Soil investigation report.

59. The verification of an element consists of comparing its characteristic resistance(s) to a design force or stress. It includes (i) a strength check where the characteristic resistance is related to the yield strength of the element; and (ii) a stability check for elements in compression where the characteristic resistance relates to the buckling limit of the element. An element (member or plate) is checked at typical sections (at least both ends and mid span) against resistance and buckling. This verification also includes the effect of water pressure for deep-water structures.
60. Ultimate limit state (ULS), which corresponds to an ultimate event considering the structural resistance with appropriate reserve

- Fatigue limit state (FLS), which relates to the possibility of failure under cyclic loading.
- Progressive collapses limit state (PLS), which reflects the ability of the structure to resist collapse under accidental or abnormal conditions.
- Service limit state (SLS), which corresponds to the criteria for normal use or durability (often specified by the plant operator).

61. 1. Calculate the vertical resultant (dead weight, live loads, and buoyancy), the overall shear and the overturning moment (environmental forces) at the mud line.
    2. Assuming that the jacket behaves as a rigid body, derive the maximum axial and shear force at the top of the pile.
    3. Select a pile diameter in accordance with the expected leg diameter and the capacity of pile-driving equipment.
    4. Derive the penetration from the shaft friction and tip bearing diagrams.
    5. Assuming an equivalent soil sub grade modulus and full fixity at the base of the jacket, calculate the maximum moment in the pile and derive its wall thickness.
62. Adapt the diameter of the leg to that of the pile, determine the effective length from the degree of fixity of the leg into the deck (depending upon the height of the cellar deck) and calculate the moment caused by wind loads on topsides and derive the appropriate thickness.
63. Select the diameter in order to obtain a span/diameter ratio between 30 and 40, calculate the axial force in the brace from the overall shear and the local bending caused by the wave assuming partial or total end restraint and derive the thickness such that the diameter/thickness ratio lies between 20 and 70 and eliminate any hydrostatic buckle tendency.
64. These loads are temporary and arise during fabrication and installation of the platform or its components. During fabrication, various structural components generate lifting forces, while in the installation phase forces are generated during platform load-out, transportation to the site, launching and upending, as well as during lifts related to installation.
65. All members and connections of a lifted component must be designed for the forces resulting from static equilibrium of the lifted weight and the sling tensions.
66. The lifting derrick or the structure to be lifted is on a floating vessel, then dynamic load factors should be applied to the static lifting forces. A factor of 2 is applied for members and connections and 1.35 for all other secondary members.
67. These are forces generated when the jacket is loaded from the fabrication yard onto the barge.
68. If the load-out is carried out by direct lift, then, unless the lifting arrangement is different from that to be used for installation, lifting forces need not be computed. This is because lifting in the open sea creates a more severe loading condition, which requires higher dynamic load factors. If load-out is done by

skidding the structure onto the barge, a number of static loading conditions must be considered, with the jacket supported on its side. Such loading conditions arise from the different positions of the jacket during the load-out phases.

69. In order to minimize the associated risks and secure safe transport from the fabrication yard to the platform site, it is important to plan the operation carefully by considering the following (API-RP2A):
    - Previous experience along the tow route
    - Exposure time and reliability of predicted "weather windows"
    - Accessibility of safe havens
    - Seasonal weather system
    - Appropriate return period for determining design wind, wave and current conditions, taking into account the characteristics of the tow such as size, structure, sensitivity, and cost.
70. It causes wave slamming forces.
71. Transporting, launching, floating, upending, straight position, pile-driving, and deck mating.
72. These forces are generated during the launch of a jacket from the barge into the sea and during the subsequent upending into its proper vertical position to rest on the seabed.
73. Five stages in a launch-upending operation are (i) jacket slides along the skid beams; (ii) jacket rotates on the rocker arms; (iii) jacket rotates and slides simultaneously; (iv) detaches completely and comes to its floating equilibrium position; and (v) jacket is upended by a combination of controlled flooding and simultaneous lifting by a derrick barge.
74. Both the static and dynamic loads for each stage of the above under the action of wind, waves, and current need to be included in the analysis.
75. As the jacket slides, its weight is supported on the two legs that are part of the launch trusses. The support length keeps decreasing and reaches a minimum, equal to the length of the rocker beams, when rotation starts. It is generally at this instant that the most severe launching forces develop as reactions to the weight of the jacket.

http://www.springer.com/978-981-10-6088-5

Dynamic Analysis and Design of Offshore Structures
Chandrasekaran, S.
2018, XXXIV, 422 p. 122 illus., 80 illus. in color.,
Hardcover
ISBN: 978-981-10-6088-5